PATENTS-US--A7184326

184,326(9)

4-21-88

S-66,627

PATENTS-US--A7184326

DE89 009602

DE-AC04-76DP00789

Douglas S. Drumheller

ACOUSTIC DATA TRANSMISSION

184,326

ACOUSTIC DATA TRANSMISSION THROUGH A DRILL STRING

INVENTOR:

DOUGLAS S. DRUMHELLER

P.O. Box 676
Cedar Crest, New Mexico 87008

ACOUSTIC DATA TRANSMISSION THROUGH A DRILL STRING

The United States Government has rights in this invention pursuant to Contract No. DE-AC04-76DP00789 between the Department of Energy and AT&T Technologies, Inc.

BACKGROUND OF THE INVENTION

This invention relates generally to a system for transmitting data along a drill string, and more particularly to a system for transmitting data through a drill string by modulation of intermediate-frequency acoustic carrier waves.

Deep wells of the type commonly used for petroleum or geothermal exploration are typically less than 30 cm (12 inches) in diameter and on the order of 2 km (1.5 miles) long. These wells are drilled using drill strings assembled from relatively light sections (either 30 or 45 feet long) of drill pipe that are connected end-to-end by tool joints, additional sections being added to the uphole end as the hole deepens. The downhole end of the drill string typically includes a drill collar, a dead weight assembled from sections of relatively heavy lengths of uniform diameter collar pipe having an overall length on the order of 300 meters (1000 feet). A drill bit is attached to the downhole end of the drill collar, the weight of the collar causing the bit to bite into the earth as the drill string is rotated from the surface. Sometimes, downhole mud motors or turbines are used to turn the bit. Drilling mud or air is pumped from the surface to the drill bit through an axial hole in the drill string. This fluid removes the cuttings from the hole, provides a hydrostatic head which controls the formation gases, and sometimes provides cooling for the bit.

Communication between downhole sensors of parameters such as pressure or temperature and the surface has long been desirable. Various methods that have been tried for this communication include electromagnetic radiation through the ground formation, electrical transmission through an insulated conductor, pressure pulse propagation through the drilling mud, and acoustic wave propagation through the metal drill string. Each of these methods has disadvantages associated with signal attenuation, ambient noise, high temperatures, and compatibility with standard drilling procedures.

The most commercially successful of these methods has been the transmission of information by pressure pulse in the drilling mud. However, attenuation mechanisms in the mud limit the transmission rate to about 2 to 4 bits per second.

This invention is directed towards the acoustical transmission of data through the metal drill string. The history of such efforts is recorded in columns 2 - 4 of U.S. Patent No. 4,293,936, issued Oct. 6, 1981, of Cox and Chaney. As reported therein, the first efforts were in the late 1940's by Sun Oil Company, which organization concluded there was too much attenuation in the drill string for the technology at that time. Another company came to the same conclusion during this period.

U.S. Patent No. 3,252,225, issued May 24, 1966, of E. Hixon concluded that the length of the drill pipes and joints had an effect on the transmission of energy up the drill string. Hixon determined that the wavelength of the transmitted data should be at least twice the length of a section of pipe.

In 1968 Sun Oil tried again, using repeaters spaced along the drill string and transmitting in the best frequency range, one with attenuation of only 10 dB/1000 feet. A paper by Thomas Barnes et al., "Passbands for Acoustic Transmission in an Idealized Drill String", Journal of Acoustical Society of America, Vol. 51, No. 5, 1972, pages 1606-1608, was consulted for an explanation of the field-test results, which were not totally consistent with the theory. Eventually, Sun went back to random searching for the best frequencies for transmission, an unsuccessful procedure.

The aforementioned Cox and Chaney patent concluded from their interpretation of the measured data obtained from a field test in a petroleum well that the Barnes model must be in error, because the center of the passbands measured by Cox and Chaney did not agree with the predicted passbands of Barnes et al. The patent uses acoustic repeaters along the drill string to ensure transmission of a particular frequency for a particular length of drill pipe to the surface.

U. S. Patent No. 4,314,365, issued February 2, 1982, of C. Petersen et al. discloses a system similar to Hixon for transmitting acoustic frequencies between 290 Hz and 400 Hz down a drill string.

U. S. Patent No. 4,390,975, issue June 28, 1983, of E. Shawhan, noted that ringing in the drill string could cause a binary "zero" to be mistaken as a "one". This patent transmitted data, and then a delay, to allow the transients to ring down before transmitting subsequent data.

U. S. Patent No. 4,562,559, issued December 31, 1985, of H. E. Sharp et al., uncovered the existence of "fine structure" within the passbands; e.g., "such fine structure is in the nature of a comb with transmission voids or gaps occurring between teeth representing transmission bands, both within the overall passbands." Sharp attributed this structure to "differences in pipe length, conditions of tool joints, and the like." The patent proposed a complicated phase shifted wave with a broader frequency spectrum to bridge these gaps.

The present invention is based upon a more thorough consideration of the underlying theory of acoustical transmission through a drill string. For the first time, the work of Barnes et al. has been analyzed as a banded structure of the type discussed by L. Brillouin, *Wave Propagation in Periodic Structures*, McGraw-Hill Book Co., New York, 1946. The theoretical results have also been correlated to extensive laboratory experiments on scale models of the drill string, and the original data tape obtained from Cox and Chaney's field-test has been reanalyzed. This analysis shows that Cox and Chaney's measurements contain data which is in excellent agreement with the theoretical predictions; that Sharp misinterpreted the cause of the fine structure; and that the ringing and the frequency limitations cited by Shawhan and Hixon are easily overcome by signal processing.

Figure 1 shows some of the results of the new analysis of the data recorded by Cox and Chaney. This figure is a plot of the power amplitude versus frequency of the transmitted signal. The theoretical boundaries between the passbands and the stopbands are shown by the vertical dotted lines. If this figure is compared to Figure 1 in Cox and Chaney's patent, significant and obvious differences can be noted. These are attributable to error in Cox and Chaney's analysis.

Furthermore, this Figure 1 also shows the "fine structure" of Sharp et al. From the new analysis we now know that this fine structure is caused by echos bouncing between opposite ends of the drill string, the number of peaks being correlated to the number of sections of drill pipe. A theoretical calculation of this field test was used to produce Figure 2. All of the phenomena important to the transmission of data in the drill string is represented in this calculation. These theoretical results accurately predict the location of the passbands and the fine structure produced by the echo phenomena.

SUMMARY OF THE INVENTION

It is an object of this invention to provide apparatus and method for transmitting data along a drill string by use of a modulated continuous acoustical carrier wave (waves) which is (are) centered within one (several) of the passbands of the drill string.

It is a further object of this invention to provide a method for transmission at carrier frequencies which are on the order of several hundreds to several thousands of Hertz in order to minimize the interference by the noise which is generated by the drilling process.

It is an additional object of this invention to provide a system for suppressing the transmission of noise within the transmission band or bands.

It is another object of this invention to provide a system for suppressing echos from the ends of the drill string.

It is still another object of this invention to provide a system for preconditioning acoustical data for transmission through a passband having characteristics determined by the parameters of the drill string.

Additional objects, advantages, and novel features of the invention will become apparent to those skilled in the art upon examination of the following description or may be learned by practice of the invention. The objects and advantages of the invention may be realized and attained by means of the instrumentalities and combinations particularly pointed out in the appended claims.

To achieve the foregoing and other objects, and in accordance with the purpose of the present invention, as embodied and broadly described herein, the present invention may comprise transmitting means for coupling data to a drill string near a first end of said drill string for acoustical transmission to a second end of said drill string; anti-noise means near the first end of said drill string for preventing acoustical noise from the first end from being transmitted through the drill string to the second end; and receiving means near the second end for receiving the acoustically transmitted data.

In addition, the invention may further comprise a method comprising the steps of preconditioning the data to counteract distortions caused by the drill string, the distortions corresponding to the effects of multiple passbands and stopbands having characteristics dependent upon the properties of the drill string; applying the preconditioned data to a first end of the drill string; and detecting the data at a second end of the drill string.

BRIEF DESCRIPTION OF THE DRAWINGS

The accompanying drawings, which are incorporated in and form part of the specification, illustrate an embodiment of the present invention and, together with the description, serve to explain the principles of the invention.

- Fig. 1 shows the measured frequency response within two passbands of the Cox-and-Chaney drill string.
- Fig. 2 shows the calculated frequency response within two passbands of the Cox-and-Chaney drill string.
- Fig. 3 shows a drill string.
- Fig. 4 shows dispersion curves for a uniform string (dashed line) and a typical drill string (solid line).

- Fig. 5 shows the transmission arrangement at a first end of a drill string.

DETAILED DESCRIPTION

As shown in Figure 3, this invention involves the transmission of acoustical data along a drill string **10** which consists of a plurality of lengths of constant diameter drill pipe **15** fastened end-to-end at thicker diameter joint portions **18** by means of screw threads as is well known in this art. Lower end **12** of drill string **10** may include a length of constant diameter drill collar to provide downward force to drill bit **22**. A constant diameter mud channel **24** extends axially through each component of drill string **10** to provide a path for drilling mud to be pumped from the surface at upper end **14** through holes in drill bit **22** as is well known in this art. The upper end **14** of drill string **10** is terminated in conventional structure such as a derrick, rotary pinion, and kelly, represented by box **25**, to permit additional lengths of drill pipe to be added to the string, and the string to be rotated for drilling. Details of this conventional string structure may be found in the aforementioned patent of E. Hixon.

Although the disclosure is directed towards transmitting data from the lower end to the upper end, it is to be understood that the teachings of this invention apply to data transmission in either direction.

The theory upon which this invention is based begins with the derivation the following Equation 1, which equation is in the form of a classical wave equation:

$$\frac{\partial^2 F}{\partial t^2} = z^2 \frac{\partial^2 F}{\partial m^2}. \tag{1}$$

where impedance $z = \rho a c$, and total axial force $F(x,t) = -cz\frac{\partial u}{\partial x}$ where ρ is density, a is area, and c is speed of sound over a cross-section of a slender, elastic, rod, u is the displacement, x is the position , m is the Lagrangian mass coordinate, and t is the time.

The existence of frequency bands which block propagation of acoustic energy is demonstrated for an idealized drill string where each piece of drill pipe consists of a tube of length d_1, mass density ρ_1, cross-sectional area a_1, speed of sound c_1, and mass r_1; and a tool joint of length d_2, mass density ρ_2, cross-sectional area a_2, speed of sound c_2, and mass r_2. A procedure demonstrated at page 180 of Brillouin has been used with the Floquet theorem to generate the following eigenvalue problem:

$$\begin{pmatrix} z_1 & z_1 & z_2 & z_2 \\ 1 & -1 & 1 & -1 \\ z_1 e^{\alpha_1 r_1} & z_1 e^{\beta_1 r_1} & z_2 e^{-\alpha_2 r_2} & z_2 e^{-\beta_2 r_2} \\ e^{\alpha_1 r_1} & -e^{\beta_1 r_1} & e^{-\alpha_2 r_2} & -e^{-\beta_2 r_2} \end{pmatrix} \begin{pmatrix} A_l/z_1 \\ B_l/z_1 \\ -A_{l-1}/z_2 \\ -B_{l-1}/z_2 \end{pmatrix} = \begin{pmatrix} 0 \\ 0 \\ 0 \\ 0 \end{pmatrix} \tag{2}$$

where

$$z_\xi = \rho_\xi a_\xi c_\xi \tag{3}$$

$$\alpha_\xi = i\,(kd/r - K_\xi) \tag{4}$$

$$\beta_\xi = i\,(kd/r + K_\xi)\ . \tag{5}$$

Here k is the wave number, $i = \sqrt{-1}$, $r = r_1 + r_2$, $d = d_1 + d_2$, $\omega = 2\pi f$, $K_\xi = \omega/z_\xi$, and f is the frequency being transmitted. This equation is seen to be similar to Equation 18 of Barnes et al., except the present examination shows Barnes' "W" to be kd.

Brillouin shows that frequencies which yield real solutions for k are banded and separated by frequency bands which yield complex solutions for k. He calls these two types of regions passbands and stopbands. The attenuation in the stopbands is generally quite large. Within each of the passbands the value of the phase velocity ω/k depends upon the value of ω. The drill string functions as an acoustic comb filter, and frequencies which propagate in the passbands are dispersed. Thus, signals which have broad frequency spectra are severely distorted by passage through a drill string. However, signal processing techniques can be used to remove this distortion.

It is to be understood that the "comb filter" referenced above refers to the gross structure in the frequency spectrum which is produced by the stopbands and the passbands, where each tooth of the comb is an individual passband. In contrast, Sharp's reference to a comb refers to a fine structure which exists within each passband.

Figure 4 shows a plot of the characteristic determinate of Equation 2 using values for ρ_ξ, a_ξ, c_ξ, and d_ξ representative of actual drill pipe parameters. The straight dotted line represents the solution for a uniform drill string, e.g., one where the diameter of the joints is equal to the diameter of the pipe. The velocity of propagation for a given frequency is represented by the phase velocity. For the uniform drill string, this ratio is constant and equal to the bar velocity of steel. When waves containing multiple frequency components travel through a uniform drill string (or drill collar **20**), they do not distort as all frequency components remain in the same relative position.

A different result occurs when the plot of Fig. 4 is curved, as each frequency then travels at a different speed. The solid lines of Fig. 4 represent the solution to Equation 2 for a realistic drill string where the area of the drill pipe is 2450 mm^2 (4 in^2) and the area of a tool joint is 12,900 mm^2 (20 in^2). In this situation, the phase velocity within each passband is curved, meaning that distortion exists.

Furthermore, the gaps represent stopbands. This analysis predicts the same values for the boundaries between the stopbands and the passbands as that of Barnes et al.; however, it also shows the characteristics of wave propagation within each of the passbands. Barnes et al. did not predict the distortion resulting from the effects of the passbands .

Calculations using a smaller diameter tool joint, representative of the reduction in diameter that occurs from wear, shows the stopbands to be narrower. This change is to be expected, because the worn joints bring the string geometry closer to the uniform geometry that produced the straight, dotted, line of Fig. 4.

Further calculations show that strings comprised of random length pipes will have significantly narrowed passbands. This result corresponds with, and for the first time explains, observations made by others.

Since the transmission of acoustical data through the drill string involves sending waves with complex transient shapes through strings of finite length, transient wave analysis has been used to predict the performance of the drill string. Fig. 2 shows the third and fourth passbands of a fast Fourier transform of the waveform which results from a signal which represents, to a rough approximation, the hammer blow used in the Cox and Chaney field test. This signal has a relatively narrow frequency content which only stimulates the third and fourth passband of the drill string. Ten sections of drill pipe were used in this field test, and the ends of the drill string produced nearly perfect reflection of the acoustic waves which resulted from the hammer blows.

This figure shows the "fine structure" of Sharp et al. to be caused by standing wave resonances within the drill string. The number of spikes in each passband correlates with the number of sections of pipe in the drill string, as explained in greater detail in the Appendix.

The analysis suggests the following technique for processing data signals and compensating for the effects of the stopbands and dispersion. First, transmit information continuously (as opposed to a broad-band pulse mode) and only within the passbands and away from the edges of the stopbands. Second, compensate for dispersion by multiplying each frequency component by $\exp(-ikL)$, where L is the transmission length in the drill pipe section **18** of the drill string. Where a large amount of acoustical noise is present, such as would be caused by a drill bit or drill mud, it is preferable to transform the data signal before transmission, resulting in an undispersed signal at the receiver position.

The foregoing analysis is based on the assumption that echos are suppressed at each end of the drill string. This is necessary to eliminate the spikes or fine structure within each of the passbands. It is common knowledge that signal processing is effective when echo strength is 20 dB below the the signal level. Each time the acoustic wave interacts with the intersection of the drill pipe and the drill collar **80**, the signal weakens by 6 dB. Also, from the analysis of Cox and Chaney's field test, the signal attenuates about 2 dB/1000 feet. Therefore, an echo which is generated by a reflection of the data signal at the top of the drill string **14** will lose $6 + 4L$ dB as it travels back down the drill string to **80** and then returns to the receiver. Thus, if the drill pipe section has a length of 3500 feet or more, the echos from the receiving end of the string will be naturally attenuated to an acceptable level.

For shorter drill strings, additional echo suppression will be required. This can be accomplished with a device called a terminating transducer. This device has an acoustical impedance which matches the acoustical impedance of the drill string and an acoustical loss factor which is sufficient to make up the required 20 dB of echo suppression.

Because attenuation in the drill string is low, the energy velocity and group velocity are approximately equal. Therefore, the characteristic impedance of the drill string is the force F divided by velocity $\frac{\partial u}{\partial t}$. This value is the eigenvalue part of Equation 2, a complex number with a real part called the viscous component and an imaginary part called the elastic component. Ideally, the terminating transducers must have a stiffness equal to the elastic component and a damping coefficient equal to the viscous component. Practically, the response need only make up the difference between 20 dB and the natural attenuation of the drill string.

The characteristic impedance is a function of frequency and position, the position dependence being periodic in accordance with the period of the drill string. Calculations show that tool joints are not a good location for a termination because the impedance is a sensitive function of position. For the fourth passband, a location 1/3 or 2/3 along the pipe is better.

The design of termination transducers is a conventional problem to those of ordinary skill in that art provided with the impedance data from Equation 2. This device, for example, could consist of a ring of polarized PZT ceramic elements and an electronic circuit whose reactive and resistive components are adjusted to tune the transducer to the characteristic impedance of the drill string and provide the necessary acoustic loss factor.

Echo suppression is a more critical problem at the downhole end of the drill string where echos travel freely up and down the drill collar section and confuse the transmission of data. At this location, it is useful to use noise cancellation techniques both to suppress echos and to prevent the noise of the drill bit or drilling mud from interfering with the desired data signal uphole. A noise cancellation technique for use with this invention is disclosed hereinafter.

Fig. 5 shows a section **30** of drill collar **20** located relatively close to downhole end **12** of drill string **10** and containing apparatus for transmitting a data signal towards the other end of the drill string while suppressing the transmission of acoustical noise up the drill string. In particular, this apparatus includes a transmitter **40** for transmitting data uphole, but not downhole, a sensor **50** for detecting acoustical noise from downhole and applying it to transmitter **40** to cancel the uphole transmission of the noise, and a sensor **60** for providing adaptive control to transmitter **40** and sensor **50** to minimize uphole transmission of noise.

Transmitter **40** includes a pair of spaced transducers **42**, **44** for converting an electrical input signal into acoustical energy in drill collar **30**. Each transducer may be a magnetostrictive ring element with a winding of insulated conducting wire. These transducers are spaced apart a distance b equal to one quarter wavelength of the center frequency of the passband selected for transmission. A data signal from source **28** is applied directly to uphole transducer **44**, preferably through a summing circuit **46**. The data signal is also applied to transducer **42** through a delay circuit **47** and an inverting circuit **48**. Delay circuit **47** has a delay value equal to distance b divided by the speed of sound in drill collar **30** at transmitter **40**.

The operation of this transmitter may be understood from the following explanation. Each of transducers **42**, **44** provide an acoustical signal F_2, F_4 that travels both uphole and downhole. Accordingly the resulting upward and downward waves from both transducers are:

$$\begin{aligned}\phi_u(t,x) &= F_2(t - x/c) + F_4(t - (x-b)/c)) \quad \text{where} \quad x > b \\ \phi_d(t,x) &= F_2(t + x/c) + F_4(t + (x-b)/c)) \quad \text{where} \quad x < 0\end{aligned} \tag{6}$$

where x is the uphole distance from transducer **42** and c is the speed of sound. For no downward wave, $\phi_d(t,x)=0$, or

$$F_2(t) = -F_4(t - b/c) \tag{7}$$

and

$$\phi_u(t,x) = -F_2(t-(x+b)/c) + F_2(t-(x-b)/c) \tag{8}$$

If the acoustical signal F_2 has the form $A\cos(\omega t)$, then Equation 8 solves to

$$\phi_u(\tau) = -2A\sin(\omega b/c)\sin(\omega\tau) \tag{9}$$

where $\tau = (t - x/c)$.

Accordingly, with a quarter wavelength spacing for waves at the center of the transmission passband, transmitter **40** transmits an uphole signal having approximately twice the amplitude A of the applied signal, and no downhole signal.

Noise sensor **50** includes a pair of spaced sensors **52**, **54** which operate in a similar manner to provide an indication of acoustic energy moving uphole, and no indication of energy moving downhole. The output of sensor **52**, which sensor may be an accelerometer or strain gauge, is an electrical signal that is summed in summing circuit **56** with the output of similar sensor **54**, which output is delayed by delay circuit **57** and and inverted by inverting circuit **58**. If the delay of circuit **57** is equal to the spacing b divided by the speed of sound c, downward moving energy is first detected by sensor **54** and delayed, and later detected by downhole sensor **52**. The inverted electrical signal from **54** arrives at summing circuit **56** at the same time as the output of sensor **52**, providing a net output of zero for downward moving noise. Upward moving noise of the form $A\sin\omega(t - x/c)$ yields an output from summing circuit **56** of:

$$\phi(t) = 2A\sin(\pi f/2f_0)\cos\omega(t - b/c) \tag{10}$$

where f_0 is the center frequency of the passband.

In the description which follows it is to be understood that all electrical signals are filtered so that the frequency content is limited to the passband or bands which are used for data transmission. Sensor **50** is spaced from transmitter **40** by distance a. Accordingly, noise that is sensed at sensor **50** arrives at transmitter **40** a time a/c later. If the output of sensors **50** is delayed by delay circuit **59** for an interval of a/c and applied to transmitter **40** through summing circuit **46**, the output of transmitter **40** can be shown to cancel the upward moving noise to within an error $\epsilon = -(\sin(\omega b/c))^2 + 1$. For a bandwidth-to-center frequency ratio of 150 Hz/650 Hz, the error is zero at the center of the transmission band and is only .03 at the band edges, a result showing 30 db noise cancellation.

Further control of upward moving noise is provided by adaptive control **70**, a conventional control circuit that has an input from a second pair of sensors **62**, **64**. These sensors, identical to sensors **52**, **54**, also have corresponding delay circuit **67** and inverter **68** to provide an output indicative of an upward moving wave and no output in response to a downward moving wave. The upward moving wave at control sensors **60** is a mixture of the noise and data that passed transmitter **40**. Accordingly, by delaying the data signal in delay circuit **72** and adding the result to the output of sensors **60** with summing circuit **74**, an error signal is produced which indicates the effectiveness of noise cancelation. This signal is fed into an adaptive control circuit **70** which controls conventional circuitry **75** to adjust voltage amplitudes or phases of the signals being applied to any of sensors **52** and **62** or transmitters **42**, **44** to minimize the amount of noise being transmitted upward towards the surface.

For a conventional steel drill collar, the spacing b between sensors or transmitters in the third passband would be about 30 cm (78 inches) or about 21 cm (53 inches) in the fourth passband.

The operation of the invention is as follows: The circuitry of Fig. 5 is mounted on a drill collar, including suitable circuitry **28** for generating data representative of a downhole parameter. Power supplies, such as batteries or mud-driven electrical generators, and other supportive circuitry known to those of ordinary skill in the art, would also be incorporated into drill collar **30**. The drill bit and mud create acoustic noise that travels in both directions through drill string **10**. Downward noise is not sensed by the sensors; however, upward noise, including echos from the bottom of the drill collar, are sensed by sensor circuit **50** and applied to transmitter circuit **40**, yielding a greatly reduced upward noise component. Primarily the data travels to the connection **80** (Fig. 3) between drill collar **30** and the lowest drill joint **18**, where a significant reflection of the data occurs because of the mismatch in acoustic impedance between these elements. Further echos occur at the tool joints **18** between each section of drill pipe **15**. These echos move downward through drill collar **30** where they pass the circuitry of Fig. 5 undetected, and become noise that is canceled out when they echo off the bottom of the drill collar. The signal that reaches the top is detected by a receiver such as an accelerometer. If necessary because of low attenuation within the drill string, an acoustically impedance matched transducer **80** may be used to terminate the signal and provide an accurate representation of the data transmitted from below.

As stated above, the data from circuit **28** may be precompensated by multiplying each frequency component of the signal by $\exp(-ikL)$ to adjust for the distortion caused by the passbands of the drill string. Such compensation may be accomplished by any manner known to those of ordinary skill in the art with a device such as an analog-to-digital signal processing circuit.

This invention recognizes and solves the problems noted by many previous workers in the field of transmitting data along a drill string. As a result, quality transmission on continuous acoustic carrier waves without extensive downhole circuitry, and without the use of impractical repeater circuits and transducers along the drill string, is possible at frequencies on the order of several hundred to several thousand Hertz. These frequencies are high in relation to the ambient drilling noise (about 1 to 10 Hz), and therefore allow transmission relatively free of this noise. Also the bandwidths of the passbands allow data rates far in excess of present mud pulse systems. Also it is recognized that this method will work in drilling situations where air is used instead of mud.

The particular sizes and equipment discussed above are cited merely to illustrate a particular embodiment of this invention. It is contemplated that the use of the invention may involve components having different sizes and shapes as long as the principle set forth in the claims is followed. It is intended that the scope of the invention be defined by the claims appended hereto. A more detailed explanation of the calculations behind this invention, and results of scale model tests and evaluations of field data, are provided in the Appendix attached to this disclosure.

Missing Page(s)
from
Original Document

ABSTRACT OF THE DISCLOSURE

Acoustical signals are transmitted through a drill string by canceling upward moving acoustical noise and by preconditioning the data in recognition of the comb filter impedance characteristics of the drill string.

DSD 4/5/88
Calculated

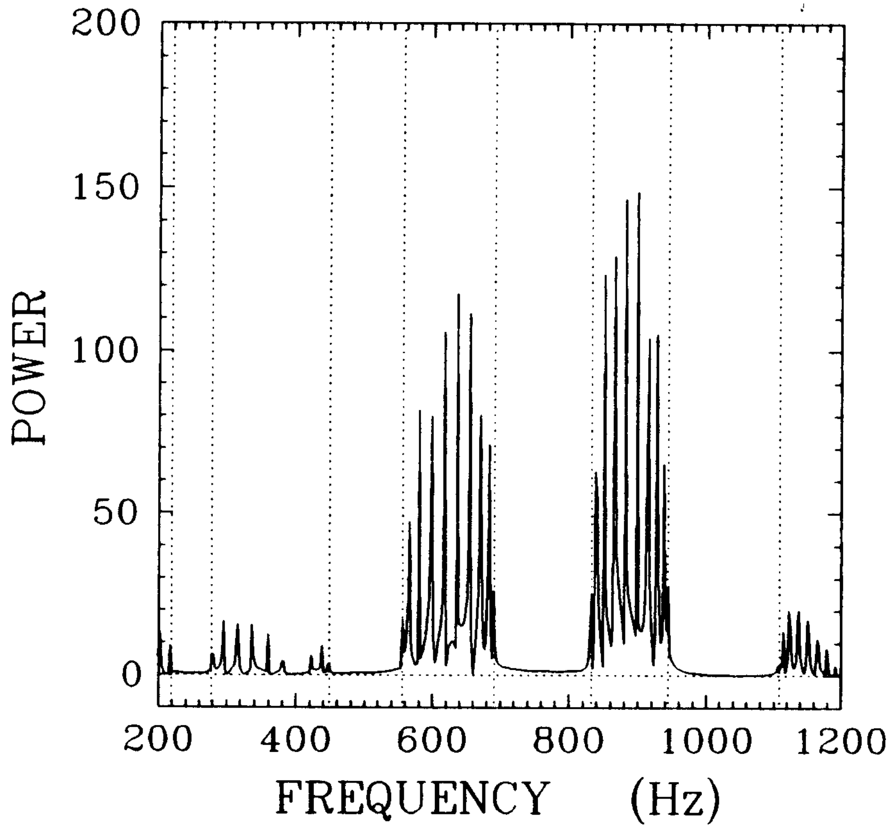

Fig. 2 DSD 4/5/88

DSD 4/5/88
Measured

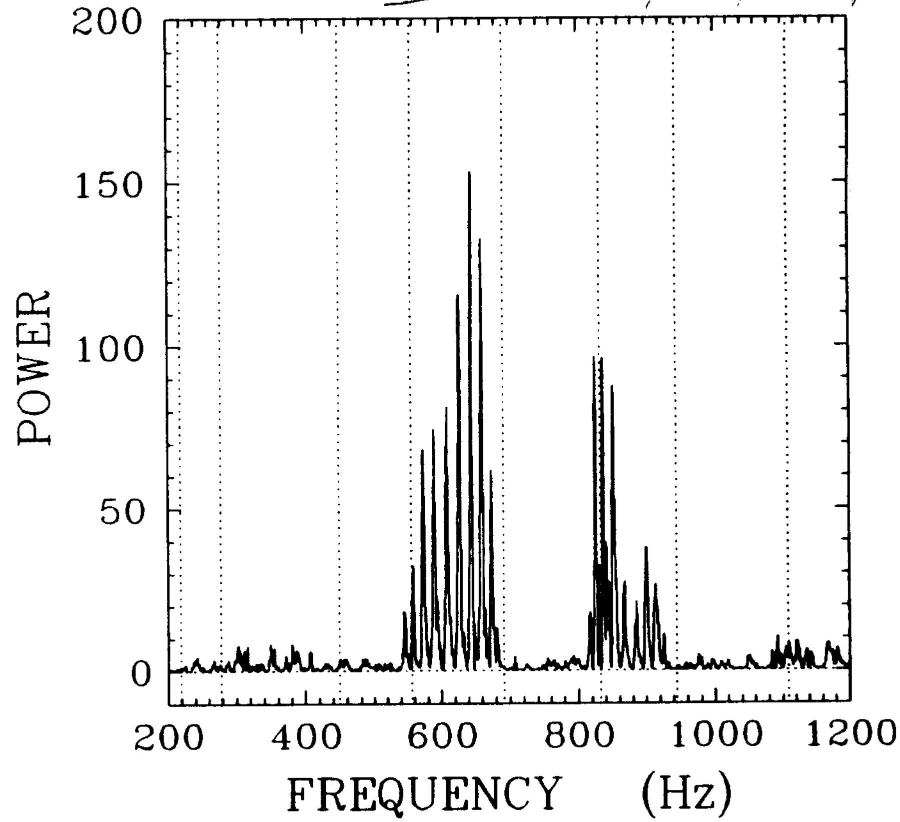

Fig. 1 DSD 4/5/88

Case No. S-66,621
Sheet 1 of 4

Case No. S-66,627
Sheet 2 of 4

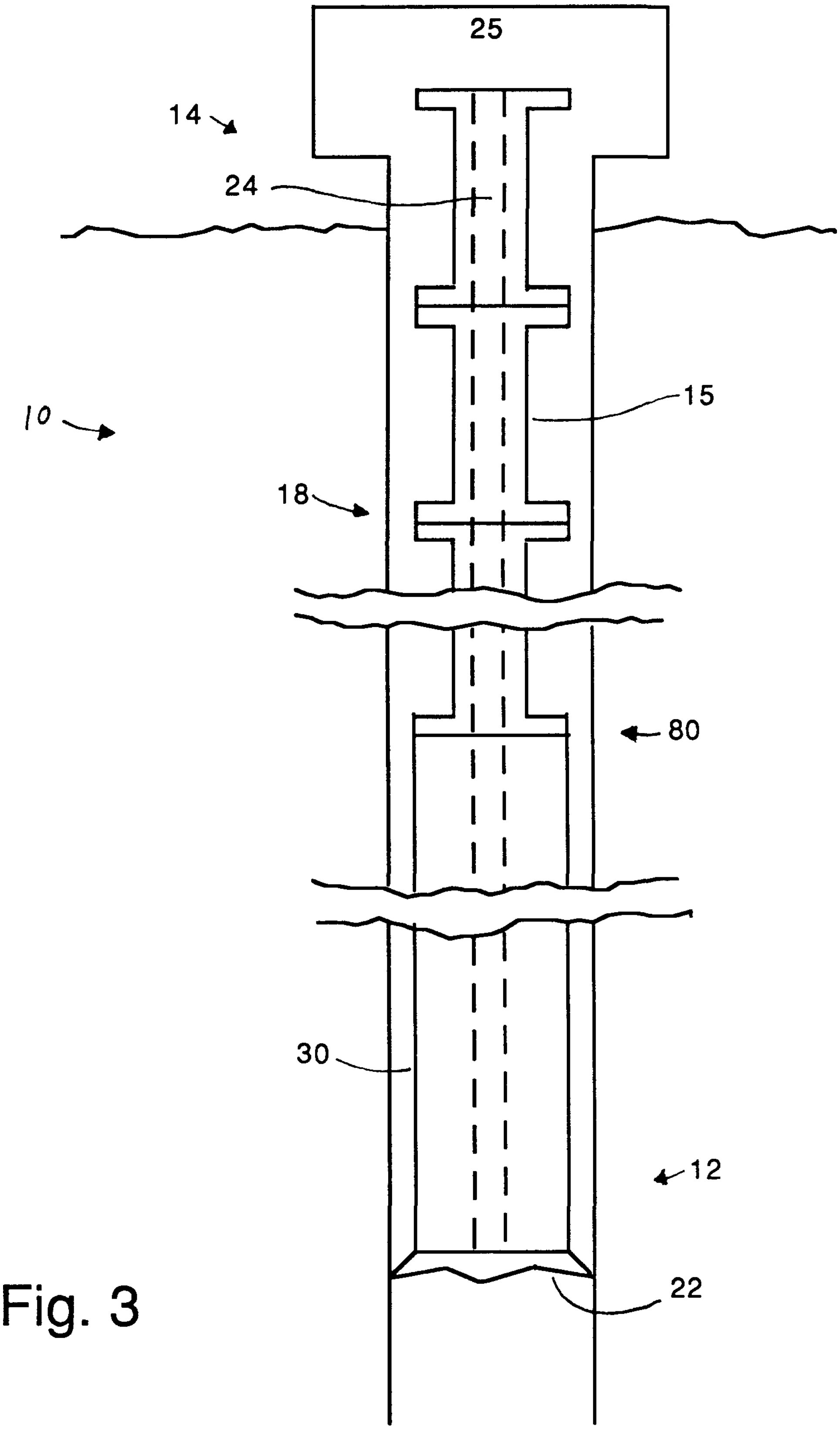

Fig. 3

Case No. S-61,627
Sheet 3 of 4

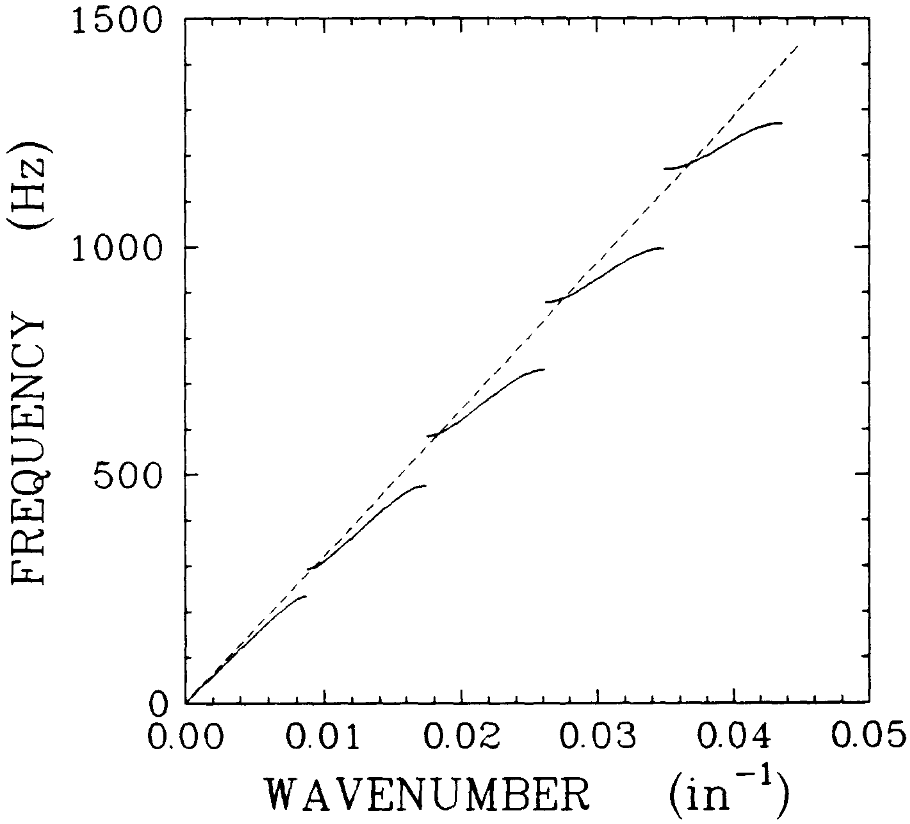

Figure 4: Disperison Curves for a Typical Drillstring.

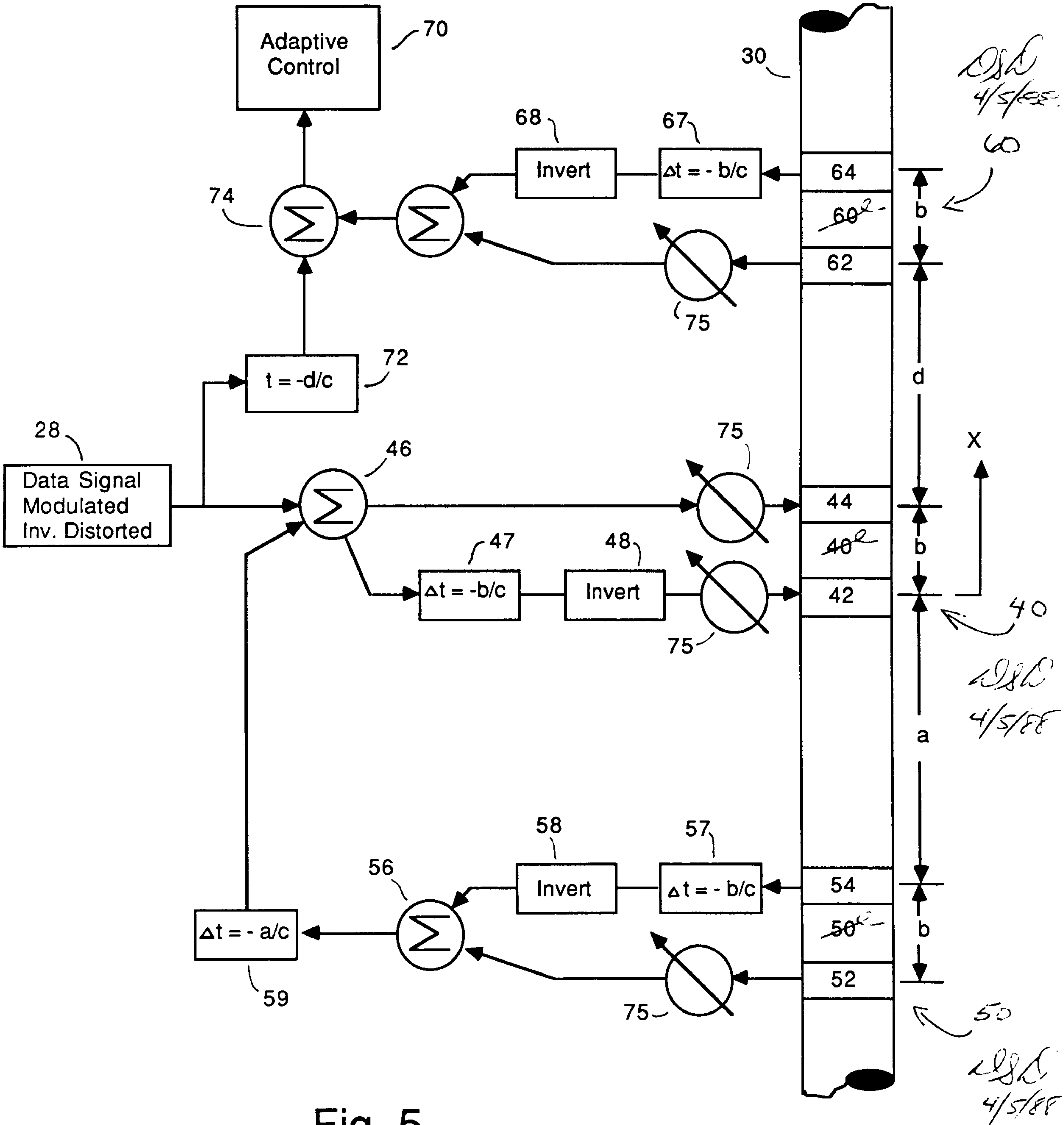
Adaptive Control
70
30
68
Invert
67
Δt = - b/c
64
60
74
b
~~60~~2
62
75
t = -d/c
72
d
28
Data Signal Modulated Inv. Distorted
46
75
X
44
47
48
b
~~40~~2
Δt = -b/c
Invert
42
75
40
a
58
57
56
Invert
Δt = - b/c
54
~~50~~2
b
Δt = - a/c
52
59
75
50

Fig. 5

Acoustical Properties of Drill Strings[1]

Douglas S. Drumheller
Geothermal Research Division
Sandia National Laboratories

ABSTRACT

The recovery of petrochemical and geothermal resources requires extensive drilling of wells to increasingly greater depths. Real-time collection and telemetry of data about the drilling process while it occurs thousands of feet below the surface is an effective way of improving the efficiency of drilling operations. Unfortunately, due to hostile down-hole environments, telemetry of this data is an extremely difficult problem. Currently, commercial systems transmit data to the surface by producing pressure pulses within the portion of the drilling mud enclosed in the hollow steel drill string. Transmission rates are between two and four data bits per second. Any system capable of raising data rates without increasing the complexity of the drilling process will have significant economic impact.

One alternative system is based upon acoustical carrier waves generated within the drill string itself. If developed, this method would accommodate data rates up to 100 bits per second. Unfortunately, the drill string is a periodic structure of pipe and threaded tool joints, the transmission characteristics are very complex and exhibit a banded and dispersive structure. Over the past forty years, attempts to field systems based upon this transmission method have resulted in little success.

This paper examines this acoustical transmission problem in great detail. The basic principles of acoustic wave propagation in the periodic structure of the drill string are examined through theory, laboratory experiment, and field test. The results indicate the existence of frequency bands which are virtually free of attenuation and suitable for data transmission at high bit rates.

[1]This work was supported by the U. S. Department of Energy at Sandia National Laboratories under Contract DE-AC04-76DP00789.

Contents

1 INTRODUCTION

Drilling deep wells is an expensive and tedious process, usually accomplished with a bit attached to a rotary drill string. This assembly may be only 5 inches in diameter and more than 5 miles long. Transducers are sometimes used to obtain direct measurement of stress, temperature, ambient gamma-ray radiation and other quantities at the bottom of the well during the drilling process. Transmitting this information to the surface is a problem of paramount importance. The various methods that have been tried include electromagnetic radiation through the rock formation, electrical transmission through an insulated conductor, pressure pulse propagation through the drilling mud, and acoustic wave propagation through the metal drill string. Each of these methods has disadvantages associated with signal attenuation, ambient noise, high temperatures, and compatibility with standard drilling procedures.

The only commercially successful method is the transmission of information by pressure pulse in the drilling mud. A severe limitation of this process is the low transmission rate, about two bits per second. Higher bit rates are precluded by attenuation mechanisms in the drilling mud.

The topic of this paper is telemetry by acoustic waves in the drill string. This method may provide the answer to attaining higher bit rates. One of the first recorded attempts to use this process was in 1948 by Sun Oil Company [1]. They performed a field test to measure acoustic attenuation in a drill string and reported a signal loss of about 12 dB/1000 ft. The test was repeated in 1968, and results showed attenuation ranging from 12 dB/1000 ft in new drill pipe to about 30 dB/1000 ft in badly worn drill pipe [1]. Several patents have been issued on devices to transmit data using this process (for examples see [1], [2], and [3]); however, the high signal losses associated with these devices have resulted in complex systems which have not found wide use.

Drill strings are assembled from 30-ft or 45-ft sections of pipe. The ends of each section have threaded tool joints with cross-sectional areas that are several times greater than the main body of the pipe. If longitudinal acoustic waves are transmitted through this structure, the acoustic impedance of this transmission line is the product of the mass density, bar velocity, and cross-sectional area of the pipe. Any spatial variation in this product along the drill string results in a partial reflection of the acoustic energy. Thus each tool joint causes multiple reflections of the data signal. At first, the number of tool joints seems to preclude this type of telemetry system; however, since the tool joints occur at periodic intervals along the length of the string, transmission is still possible within discretely spaced frequency bands.

A theoretical analysis of an idealized drill string was presented by Barnes and Kirkwood in 1972 [4]. They demonstrated the complexity of this wave propagation problem by identifying its banded frequency structure. Waves propagate without attenuation in half of the bands (passbands), and each of these bands is separated by a region where attenuation is very high (stopbands).

This theoretical work was known to those who were trying to develop a transmission system. Discrepancies between field measurements and theoretical predictions were reported [1]. Also a *fine structure* was noted within the frequency spectrum of each of the passbands [2], and attributed to imperfections in the tool joints. Unfortunately, no laboratory data was obtained for comparison to the theory. Furthermore the work of Barnes and Kirkwood only predicted the boundaries between the passbands and stopbands. The behavior of waves within each of the passbands was not investigated.

In Section 2 a detailed analysis of the transmission characteristics of a drill string is presented. The results of this analysis show the relationship of this problem to the classical Brillouin wave scattering problem [5]. In addition to the passbands and stopbands, the results show that within each passband, large amounts of wave dispersion are present. Complex resonance effects result not only from the tool joints, but also from the finite length of the drill string. Both these effects combine to produce a complex spike pattern or *fine structure* in the frequency spectrum of each passband. These are the phenomena reported in [2]. This section concludes with a description of a method of transmission which circumvents the problem of wave dispersion in the passbands.

Section 3 contains the description of a laboratory experiment. The acoustical transmission characteristics of a 20th-scale model of a drill string are studied. The purpose of this experiment is two fold: first, to produce a carefully controlled experimental data base for comparison to the theory; and second to develop a scale model as a tool for evaluating designs for the sending and terminating transducers of a telemetry system. Very good comparisons are achieved between theory and experiment.

In Section 4, the relevance of the theory and the laboratory experiment to the actual field environment is investigated. An analysis of a field test performed in 1975 by **Sun Oil Company** is presented. The influences of real drill pipe with low dimensional tolerances, tool joints with complex geometry, and drill string assemblies which are submerged in drilling mud are examined. It is concluded that both the theory and laboratory experiment are in close agreement with these field results: attenuation in the actual field situation is supprisingly low, less than 4 dB/1000 ft; and the major difficulty in designing a telemetry system is not overcoming signal attenuation, but rather suppressing echos and background noise.

2 THEORY

A theory is developed to study acoustical wave propagation in a drill string. The model described in Section 2.1 is one dimensional and linear. Section 2.2 contains the analysis of periodic acoustic disturbances. It is based upon a method of analysis presented by Brillouin [5] more than forty years ago. Examination of Brillouin's work reveals similarities of this problem to many other problems including electrical transmission lines, X-ray defraction, and wave propagation in composite materials [6]. Transient waves in a drill string of finite length are analyzed in Section 2.3. Section 2.4 contains a description of the calculated results.

2.1 The Model

In this section the propagation of plane longitudinal waves along the length of a slender elastic rod is considered. The position along the rod will be denoted by the variable x. Time is denoted by t. The properties of this rod which are important to the present problem are the initial mass density $\rho(x)$, the initial cross-sectional area $a(x)$, and Young's modulus $E(x)$. These quantities are assumed to be functions of position alone. They are not affected by acoustic disturbances, and therefore are not functions of time. In a slender rod the relationship between the axial stress $\sigma(x,t)$, taken positive in compression, and displacement $u(x,t)$ is given by

$$\sigma = -E\frac{\partial u}{\partial x}. \tag{1}$$

If the sound speed $c(x)$ is defined as

$$c^2 = \frac{E}{\rho}, \tag{2}$$

then the total axial force $F(x,t)$ acting over a cross-section of the rod can be written as

$$F = -\rho a c^2 \frac{\partial u}{\partial x}. \tag{3}$$

The equation of motion for the rod is

$$\rho a \frac{\partial v}{\partial t} = -\frac{\partial F}{\partial x} \tag{4}$$

where the particle velocity $v(x,t)$ is defined by

$$v = \frac{\partial u}{\partial t}. \tag{5}$$

In these relations the independent variables are time and position. It is useful to define another coordinate, the mass coordinate m, to replace the position coordinate x. The mass coordinate is defined by

$$m = \int_0^x \rho(\zeta)a(\zeta)d\zeta. \tag{6}$$

From Eq. 6

$$\frac{\partial}{\partial x} = \rho a \frac{\partial}{\partial m}. \tag{7}$$

Equations 3 and 4 can now be rewritten as

$$
\begin{aligned}
F &= -z^2 \frac{\partial u}{\partial m} && (8) \\
\frac{\partial v}{\partial t} &= -\frac{\partial F}{\partial m} && (9)
\end{aligned}
$$

where the impedance z is defined as

$$z = \rho a c \; . \tag{10}$$

Equations 8 and 9 can be combined to yield

$$
\begin{aligned}
\frac{\partial^2 u}{\partial t^2} &= \frac{\partial}{\partial m}\left(z^2 \frac{\partial u}{\partial m}\right) && (11) \\
\frac{\partial^2 F}{\partial t^2} &= z^2 \frac{\partial^2 F}{\partial m^2}. && (12)
\end{aligned}
$$

Equation 12 is in the form of a classical wave equation. This has important implications for the following development.

2.2 Dispersion Analysis

In this section the behavior of time harmonic waves in an infinitely long drill string is investigated. The existence of frequency bands which block propagation of acoustic energy is demonstrated. These bands are separated by regions which pass energy; however, within the passbands different frequencies propagate at different speeds and produce distortion of the signal.

The analysis begins by taking the Fourier transform of Eqn. 12. For zero initial conditions, the result is

$$\frac{d^2 \mathcal{F}}{dm^2} + K^2 \mathcal{F} = 0 \tag{13}$$

where $\mathcal{F}(m, \omega)$ is the transform of $F(m,t)$, ω is the circular frequency, and

$$K = \frac{\omega}{z} \; . \tag{14}$$

In the special case when $K(m, \omega)$ is a periodic function of m, Eqn. 13 is in the form of Hill's equation. The Floquet theorem applies to this problem. This theorem states that solutions can be written in the form

$$\mathcal{F} = f(m, \omega) \exp(-i\gamma m) \tag{15}$$

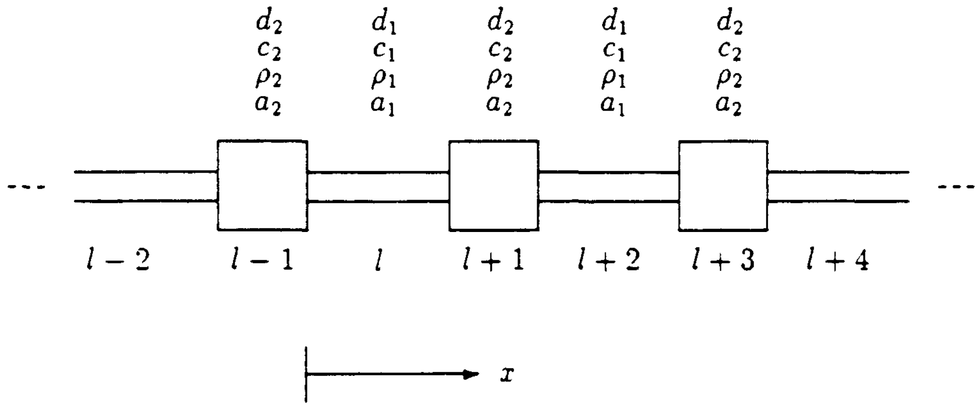

Figure 1: The Idealized Drill String Geometry.

where $f(m,\omega)$ is a periodic function of m with a period equal to $K(m,\omega)$.

For the idealized drill string illustrated in Figure 1, $K(m,\omega)$ is clearly a periodic function of m. This string is composed of two types of elements. The properties of each element are constant and labeled with the subscript ξ where $\xi = 1, 2$. The length of each element is denoted by d_ξ. The mass of each element is denoted by r_ξ where

$$r_\xi = \rho_\xi a_\xi d_\xi \ . \tag{16}$$

The periodic length of the string in terms of length x is denoted by d and in terms of mass m is denoted by r where

$$d = d_1 + d_2 \tag{17}$$

$$r = r_1 + r_2 \ . \tag{18}$$

Within each element, K is a constant denoted by K_ξ where

$$K_\xi = \frac{\omega}{\rho_\xi a_\xi c_\xi} \ . \tag{19}$$

The solution to this problem can be obtained through a procedure demonstrated by Brillouin ([5], p. 180). It is first noted that in an given element s of the drill string the solution to Eqn. 13 is

$$\mathcal{F}_s = A_s \exp(-iK_\xi m) + B_s \exp(iK_\xi m) \ , \tag{20}$$

where $i^2 = -1$. This solution can be rewritten into the form of Eqn. 15 to obtain

$$\mathcal{F}_s = f_s(m, \omega) \exp(-ikmd/r) \ , \tag{21}$$

where

$$f_s(m, \omega) = A_s \exp i\,(kd/r - K_\xi)\, m + B_s \exp i\,(kd/r + K_\xi)\, m \ . \tag{22}$$

From the transform of Eqn. 9,

$$\mathcal{V}_s = \frac{1}{z_\xi} g_s(m, \omega) \exp(-ikmd/r) \ , \tag{23}$$

where

$$g_s(m, \omega) = A_s \exp i\,(kd/r - K_\xi)\, m - B_s \exp i\,(kd/r + K_\xi)\, m \ . \tag{24}$$

The function $\mathcal{V}_s(m, \omega)$ is the transform of $v(m, t)$ in element s.

Each of the functions $f_s(m, \omega)$ and $g_s(m, \omega)$ is a piece of a periodic function, $f(m, \omega)$ and $g(m, \omega)$. The solutions for each element are connected together through sets of boundary conditions at each of the element joints. The Floquet theorem provides a method for evaluating these functions by considering only two adjacent sets of boundary conditions. For convenience, the joints at $x = 0$ and $x = d_1$ in Figure 1 are used. At both joints it is required that the force and the motion are continuous. Therefore,

$$\begin{aligned} \mathcal{F}_{l-1}(0, \omega) &= \mathcal{F}_l(0, \omega) && (25)\\ \mathcal{V}_{l-1}(0, \omega) &= \mathcal{V}_l(0, \omega) && (26)\\ \mathcal{F}_l(r_1, \omega) &= \mathcal{F}_{l+1}(r_1, \omega) && (27)\\ \mathcal{V}_l(r_1, \omega) &= \mathcal{V}_{l+1}(r_1, \omega) \ , && (28) \end{aligned}$$

which is a set of four equations in six unknowns. Substitution of Eqns. 21 and 23, and application of the Floquet theorem gives

$$\begin{aligned} f_{l-1}(0, \omega) &= f_l(0, \omega) && (29)\\ \frac{1}{z_2} g_{l-1}(0, \omega) &= \frac{1}{z_1} g_l(0, \omega) && (30)\\ f_{l-1}(-r_2, \omega) &= f_l(r_1, \omega) && (31)\\ \frac{1}{z_2} g_{l-1}(-r_2, \omega) &= \frac{1}{z_1} g_l(r_1, \omega) \ , && (32) \end{aligned}$$

which is a set of four equations in four unknowns.

Equations 29 through 32 result in the following eigenvalue problem:

$$\begin{pmatrix} z_1 & z_1 & z_2 & z_2 \\ 1 & -1 & 1 & -1 \\ z_1 e^{\alpha_1 r_1} & z_1 e^{\beta_1 r_1} & z_2 e^{-\alpha_2 r_2} & z_2 e^{-\beta_2 r_2} \\ e^{\alpha_1 r_1} & -e^{\beta_1 r_1} & e^{-\alpha_2 r_2} & -e^{-\beta_2 r_2} \end{pmatrix} \begin{pmatrix} A_l/z_1 \\ B_l/z_1 \\ -A_{l-1}/z_2 \\ -B_{l-1}/z_2 \end{pmatrix} = \begin{pmatrix} 0 \\ 0 \\ 0 \\ 0 \end{pmatrix} \qquad (33)$$

where

$$\alpha_\xi = i\,(kd/r - K_\xi) \qquad (34)$$

$$\beta_\xi = i\,(kd/r + K_\xi)\ . \qquad (35)$$

For a nontrivial solution to exist, the determinant of the square matrix in Eqn. 33 must equal zero. This condition is satisfied when

$$\cos kd = \cos\left(\frac{\omega d_1}{c_1}\right)\cos\left(\frac{\omega d_2}{c_2}\right) - \frac{1}{2}\left(\frac{z_1}{z_2} + \frac{z_2}{z_1}\right)\sin\left(\frac{\omega d_1}{c_1}\right)\sin\left(\frac{\omega d_2}{c_2}\right)\ . \quad (36)$$

For the special case when $z_1 = z_2$, the solution to Eqn. 36 is

$$\frac{kd}{\omega} = \frac{d_1}{c_1} + \frac{d_2}{c_2}\ , \text{for } z_1 = z_2\ . \qquad (37)$$

Also when the drill string is uniform so that $z_1 = z_2$ and $c_1 = c_2 = c$, the solution is

$$c = \frac{\omega}{k}\ , \text{for a uniform string.} \qquad (38)$$

Equation 36 is similar to Eqn. 18 in Barnes and Kirkwood [4]. The major difference is in the comparisons of the left-hand sides. Barnes and Kirkwood's relation contains the term $\cos W$. They claim that W must be real for *lossless transmission*. The present analysis shows that $W = kd$. Real values of W correspond to real values of the wavenumber k. Examination of Eqn. 21 shows that real values of k indeed correspond to solutions which propagate without attenuation. Brillouin discusses Eqn. 36 in great detail. He shows that frequencies which yield real solutions for k are banded and separated by frequencies which yield complex solutions for k. He calls these two types of regions passbands and stopbands. The attenuation in the stopbands is generally quite large. Within each of the passbands the value of the phase velocity ω/k depends upon the value of ω. The drill string functions as a comb filter, and frequencies which propagate in the passbands are dispersed. Thus signals which have broad frequency spectra are severely distorted. Transmission of information by acoustic signal through the drill string is severely limited unless signal processing is used to remove this distortion. The nature of this signal distortion will be examined more fully in Section 2.4.

2.3 Transient Analysis

Two methods for analyzing the behavior of transient waves in a drill string are the method of characteristics and the finite-difference technique. Under the special situations described here, these two approaches are equivalent and result in an efficient method for analyzing the response of a drill string of finite length.

It is first required that the ratio $\mathcal{R}$,

$$\mathcal{R} = \frac{d_1/c_1}{d_2/c_2} = \frac{n_1}{n_2} , \tag{39}$$

is a rational number; that is, n_1 and n_2 are integers. It is then possible to choose a time increment Δt so that

$$d_1 = c_1 n_1 \Delta t \tag{40}$$

$$d_2 = c_2 n_2 \Delta t \tag{41}$$

The length coordinate can then be overlayed with mesh points x_n so that the interval

$$\Delta x_{n+\frac{1}{2}} = x_{n+1} - x_n \tag{42}$$

is equal to either d_1/n_1 or d_2/n_2, depending upon the element of the drill string in which $\Delta x_{n+\frac{1}{2}}$ is located. Within each of these intervals the mass density, sound speed, and cross-sectional area are constant and denoted by $\rho_{n+\frac{1}{2}}$, $c_{n+\frac{1}{2}}$, and $a_{n+\frac{1}{2}}$. From Eqn. 16

$$\Delta r_{n+\frac{1}{2}} = \rho_{n+\frac{1}{2}} a_{n+\frac{1}{2}} \Delta x_{n+\frac{1}{2}} . \tag{43}$$

This system of mesh points can now be used to either develop a finite-difference algorithm for the solution of Eqn. 11 or it can be used to trace characteristic solutions. It is possible to use this system to trace characteristics since the mesh spacing has been chosen so that all waves require a time of Δt to travel from one mesh point to a neighboring mesh point. Thus, if the initial and boundary conditions to the problem result only in shock increments located at mesh points for times which are integer multiplies of Δt, then all characteristics simultaneously intersect the mesh points only at integer multiplies of Δt. The finite-difference algorithm is developed first, and its connection to the method of characteristics is then examined.

The displacement field $u(x, t)$ is approximated by a discrete set of values u_n^j where j and n denote the value at time $j\Delta t$ and position x_n. By using simple-centered finite differences, the velocity, and acceleration are [7]

$$\left(\frac{\partial u}{\partial t}\right)_n^{j+\frac{1}{2}} = \left(u_n^{j+1} - u_n^j\right)/\Delta t \tag{44}$$

$$\left(\frac{\partial^2 u}{\partial t^2}\right)_n^j = \frac{1}{\Delta t}\left[\left(\frac{\partial u}{\partial t}\right)_n^{j+\frac{1}{2}} - \left(\frac{\partial u}{\partial t}\right)_n^{j-\frac{1}{2}}\right]$$
$$= \left(u_n^{j+1} - 2u_n^j + u_n^{j-1}\right)/\Delta t^2 \ . \quad (45)$$

Equation 11 becomes

$$u_n^{j+1} \ -2u_n^j + u_n^{j-1} =$$
$$\frac{2(\Delta t)^2}{\Delta r_{n+\frac{1}{2}} + \Delta r_{n-\frac{1}{2}}}\left[z_{n+\frac{1}{2}}^2\left(\frac{u_{n+1}^j - u_n^j}{\Delta r_{n+\frac{1}{2}}}\right) - z_{n-\frac{1}{2}}^2\left(\frac{u_n^j - u_{n-1}^j}{\Delta r_{n-\frac{1}{2}}}\right)\right] \quad (46)$$

By noting that

$$z_{n+\frac{1}{2}} = \rho_{n+\frac{1}{2}} a_{n+\frac{1}{2}} c_{n+\frac{1}{2}} = \Delta r_{n+\frac{1}{2}}/\Delta t \ . \quad (47)$$

the following finite-difference algorithm is obtained:

$$u_n^{j+1} + u_n^{j-1} = \frac{2\Delta r_{n+\frac{1}{2}}}{\Delta r_{n+\frac{1}{2}} + \Delta r_{n-\frac{1}{2}}} u_{n+1}^j + \frac{2\Delta r_{n-\frac{1}{2}}}{\Delta r_{n+\frac{1}{2}} + \Delta r_{n-\frac{1}{2}}} u_{n-1}^j \ . \quad (48)$$

To illustrate the connection of this relationship to the method of characteristics. the results for an incident wave interacting with a material impedance change at mesh point n are used [8]. For an incident wave U_I traveling in the positive x direction. the resulting reflected wave U_R and transmitted wave U_T are (see Zel'dovich and Raizer [8])

$$U_R = \frac{\Delta r_{n-\frac{1}{2}} - \Delta r_{n+\frac{1}{2}}}{\Delta r_{n-\frac{1}{2}} + \Delta r_{n+\frac{1}{2}}} U_I \quad (49)$$
$$U_T = \frac{2\Delta r_{n-\frac{1}{2}}}{\Delta r_{n-\frac{1}{2}} + \Delta r_{n+\frac{1}{2}}} U_I \ , \quad (50)$$

and for an incident wave traveling the negative x direction

$$U_R = \frac{\Delta r_{n+\frac{1}{2}} - \Delta r_{n-\frac{1}{2}}}{\Delta r_{n-\frac{1}{2}} + \Delta r_{n+\frac{1}{2}}} U_I \quad (51)$$
$$U_T = \frac{2\Delta r_{n+\frac{1}{2}}}{\Delta r_{n-\frac{1}{2}} + \Delta r_{n+\frac{1}{2}}} U_I \ . \quad (52)$$

Since all incident waves only interact with mesh points at times $j\Delta t$, these relations are only required for computations at positions x_n and times $j\Delta t$. It is a straightforward, although jejune, exercise to demonstrate that Eqn. 48 is equivalent to repeated application of Eqn. 49 through 52 for all possible combinations of waves at time $(j-1)\Delta t$ which could affect the solution at time $(j+1)\Delta t$ and position x_n.

This special choice of mesh spacing has another advantage. The time increment Δt is called the critical time step [7]. For other problems in which the meshes are not spaced by the critical time step, instabilities and oscillations are produced by the numerical algorithm. An artificial viscosity term is normally employed to dampen these oscillations. Because of the special nature of the present problem which allows this uniform spacing in time, the calculations do not exhibit these numerical artifacts and artificial viscosity is not required.

Boundary conditions must also be specified at the left and right boundaries of the drill string. Either the displacement u_n^j or the force $F_{n-\frac{1}{2}}^j$ can be specified.

The force boundary condition requires the differenced form of Eqn. 3 which is

$$F_{n-\frac{1}{2}}^j = \Delta r_{n-\frac{1}{2}} \left(u_{n-1}^j - u_n^j\right) / \Delta t^2 \ . \tag{53}$$

The displacement boundary condition can also be used to produce the effect of an infinite uniform material extending beyond the boundary position. The resulting boundary conditions are

$$u_n^j = \begin{cases} \mathcal{U}_n^j & \text{displacement} \\ \dfrac{(\Delta t)^2 \mathcal{T}_{n+\frac{1}{2}}^j}{\Delta r_{n+\frac{1}{2}}} + u_{n+1}^j & \text{left force} \\ -\dfrac{(\Delta t)^2 \mathcal{T}_{n-\frac{1}{2}}^j}{\Delta r_{n-\frac{1}{2}}} + u_{n-1}^j & \text{right force} \\ u_{n+1}^{j-1} & \text{left infinite} \\ u_{n-1}^{j-1} & \text{right infinite} \end{cases} \tag{54}$$

The functions $\mathcal{U}_n^j$, $\mathcal{T}_{n+\frac{1}{2}}^j$, and $\mathcal{T}_{n-\frac{1}{2}}^j$ are arbitrary functions describing the applied displacements and forces at the boundaries of the problem.

Equation 48 is used to compute the transient response of the drill string. If the string extends from $n = 0$ to $n = N$, then u_n^0 and u_n^1 is specified for $n = 0, \ldots, N$. This is equivalent to specifying the initial values of displacement and velocity of the drill string. Equation 48 is then used to compute values of u_n^2 for $n = 1, \ldots, N-1$ and Eqn. 54 is used to compute values for u_0^2 and u_N^2. The process is repeated for increasing values of j.

2.4 Acoustic Phenomena

The preceding sections contain the development of a model for a drill string and the analysis for both periodic waves in a drill string of infinite length and transient waves in

Table 1: Drill String Parameters

parameter	pipe		tool joint	
	regular	long	new	used
a_ξ	3.80 in^2	3.80 in^2	20.0 in^2	13.1 in^2
d_ξ	342 in	360 in	18.0 in	18.0 in

a drill string of finite length. In this section, results are presented for a representative steel drill string. A specific gravity of 7.87 and a bar velocity of 202,000 in/s are used. The other parameters necessary for these calculations are listed in Table 1. [2] Note that the cross-sectional area and therefore the total mass of the tool joints decreases approximately 35 percent during normal usage. This reduction is due to abrasion of the tool joints by the natural formation and the well casing. Both new and used pipe are included to illustrate the effects of wear upon the acoustic dispersion characteristics. The effects of length are also illustrated with both regular and long drill pipe.

For clarity, this section begins by examining the response of a uniform drill string in which the cross section of the tool joints is equal to that of the drill pipe. The solution to Eqn. 36 for this case is illustrated by the straight dashed line in Figure 2. This is a plot of real wavenumber k versus frequency ω. The velocity of propagation of a given frequency is represented by the ratio ω/k which is called the phase velocity. For the uniform drill string, this ratio is constant and equal to the bar velocity of steel as given by Eqn. 2. When waves which contain multiple frequency components travel through this string, they do not distort since all frequency components remain in the same relative position; however, when curvature is present in this plot, each frequency travels at a different speed, and distortion results. For this reason these plots are called dispersion curves.

The dispersion curves for the new drill string with regular length pipe are also shown in Figure 2. Unlike the uniform drill string, curvature is present. Also, gaps exist. These are frequency bands in which the wavenumber is complex, indicating attenuation. The curves represent passbands, and the gaps represent stopbands.

Although an infinite number of passbands exist, only the first five are shown here. The first passband ends at a frequency of 235 Hz. The wavenumber at this frequency is $k = \pi/d$; that is, the wavelength is twice the periodic length of the string. The other boundaries occur at integer multiples of this wavenumber. For a given frequency, Eqn. 36 yields multiple solutions for k. Each produces an identical waveform within the drill string. For this reason the additional solutions within the passbands are not

[2] These parameters represent 4-in nominal, steel drill pipe which weighs 14 lbs/ft with 4-in, grade X95, steel tool joints. The new and used tool joints in this table conform to class I and class III American Petroleum Institute specifications [9].

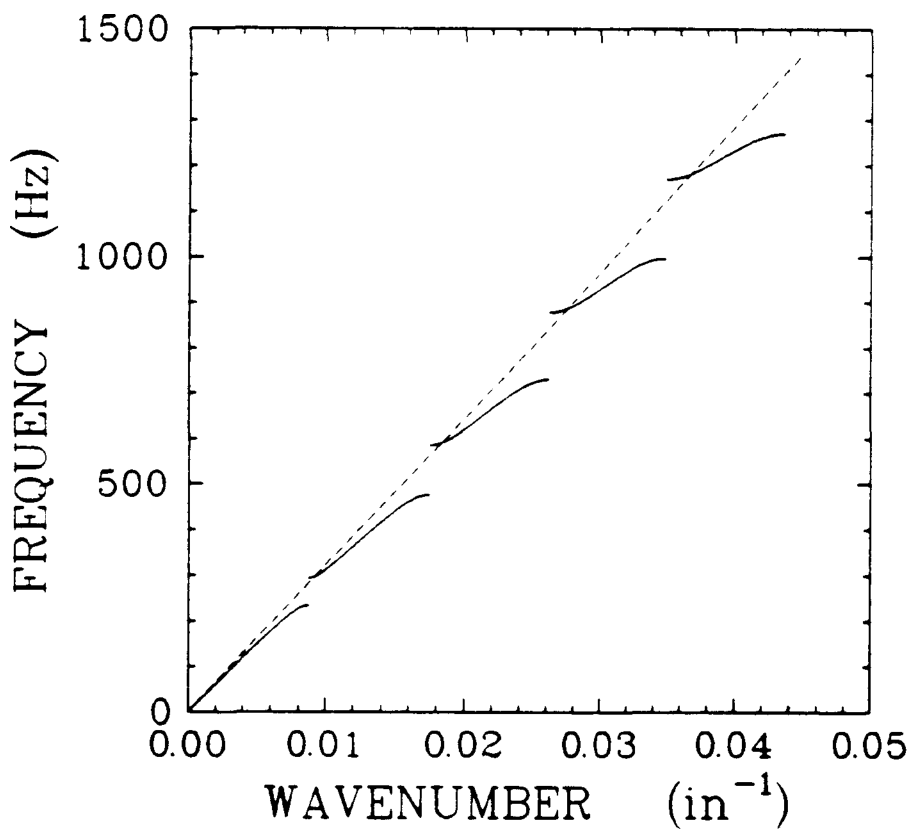

Figure 2: Dispersion Curves for New Drill String (Solid Line) and Uniform String (Dashed Line).

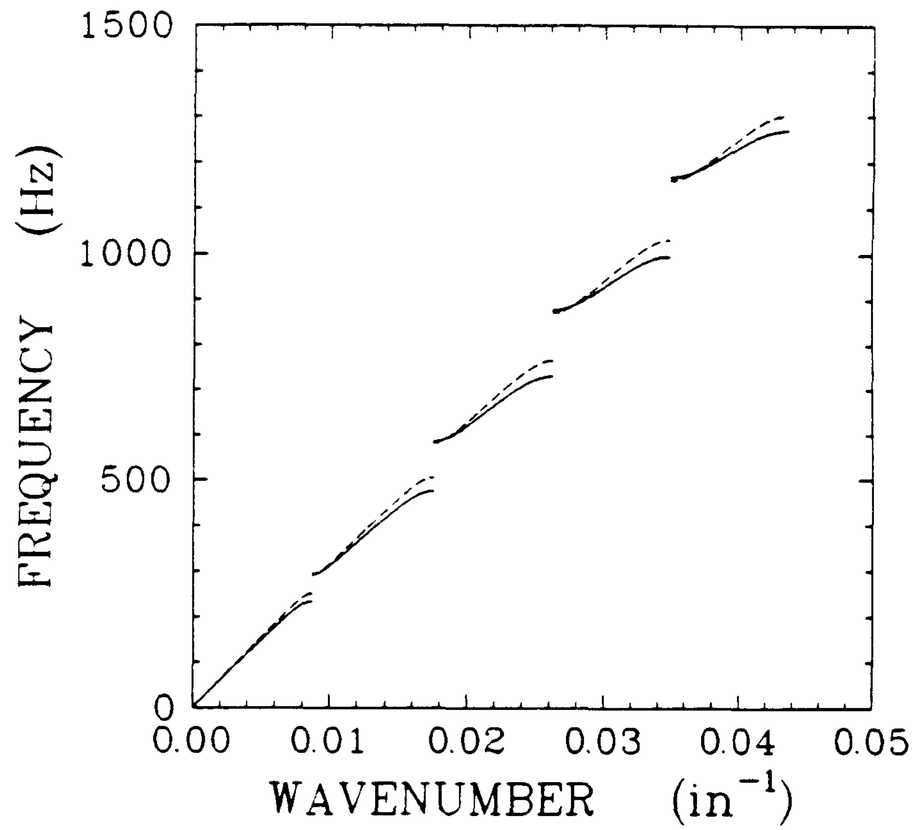

Figure 3: Dispersion Curves for New Drill String (Solid Line) and Old Drill String (Dashed Line).

plotted. This multivalued characteristic of the solutions is discussed in detail in [5].

For a linear problem, a transient wave can be decomposed into its frequency components. Many times, the dominant frequency components are grouped together into one or more bands. Instead of propagating at the phase velocity, each of these groups of waves propagates with a velocity determined by the slope of the dispersion curve. $d\omega/dk$, evaluated at the center frequency of the band. This is called the group velocity. When attenuation is low, it represents the speed of propagation of the energy contained in the group of waves. The group velocity and the phase velocity are constant and equal in the uniform string. In the new drill string, they are different and both are functions of frequency.

Figure 3 shows the dispersion curve for the old drill string and its comparison to the new drill string. The effect of the reduced cross-sectional area of the tool joints is obvious. The stopbands are narrower. There is also a significant change in the predicted group velocities for the old drill string. The process of wear has a pronounced influence upon the transmission characteristics.

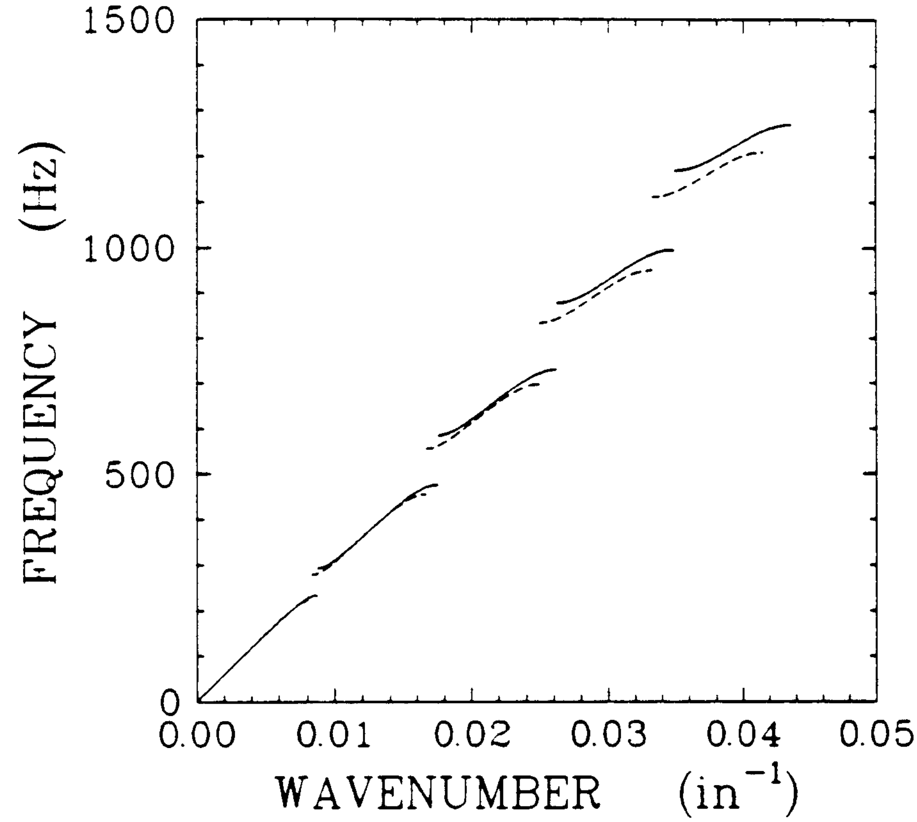

Figure 4: Dispersion Curves for New Drill String (Solid Line) and Long Drill String (Dashed Line).

Figure 4 shows the comparison of the new drill string with regular length pipe to the new drill string with long pipe. Again, a significant influence can be seen in the comparison. This suggests that drill strings composed of random lengths of pipe have significantly narrowed passbands.

Telemetry of data involves transmitting waves with complex transient shapes through drill strings of finite length. A clearer understanding of the relationship of the dispersion curves to this problem is obtained by using the algorithm developed in Section 2.3.

Both the old and new drill strings are divided into the same number of mesh intervals. For the tool joints, $n_1 = 1$, and for the pipe, $n_2 = 19$ (see Eqn. 39). In the calculations, 9 pipe elements separated by 10 tool joints are used. Also a long element of drill pipe is included between the left boundary of the problem and the beginning of the drill string. This long element is included to isolate the left boundary from the influences of the tool joints; that is, the left boundary is effectively at an infinite distance from the beginning of the drill string. A specified velocity condition of unit amplitude is used for at left boundary, and an infinite material condition is used at the

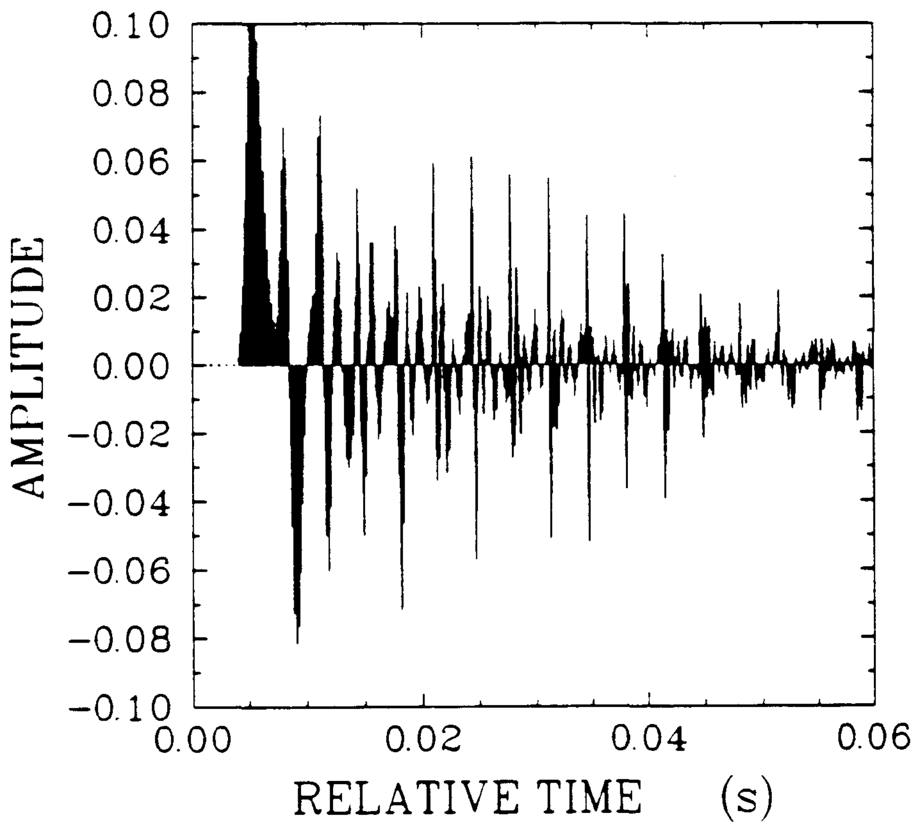

Figure 5: Impulse Response of 9 Segments.

right boundary.

The first calculation illustrates the response of the new drill string with regular length pipe to an impulse of unit amplitude. An infinitely narrow impulse contains a frequency spectrum with equal amounts of all frequencies. If the frequency content of the transmitted wave is examined at the right boundary, the response of the drill string to all frequencies is determined.

Because of the finite-differencing algorithm used in these calculations, the input pulse cannot be infinitely narrow but must have a minimum width of $\Delta t = 89\ \mu s$. The transmitted wave which results from this impulse is shown in Figure 5. The waveform is a burst of rapid oscillations which has a significant amplitude for a large fraction of second. If a Fast Fourier Transform is taken of this waveform, the frequency spectrum in Figure 6 is obtained.[3] The dashed line is the spectrum of the input pulse. This plot clearly shows that after traveling through only nine segments of drill pipe, all but the lowest of the stopbands have effectively blocked their frequency components.

[3] This transform was made using a sampling interval of $\Delta t = 89\ \mu s$ and 8192 points.

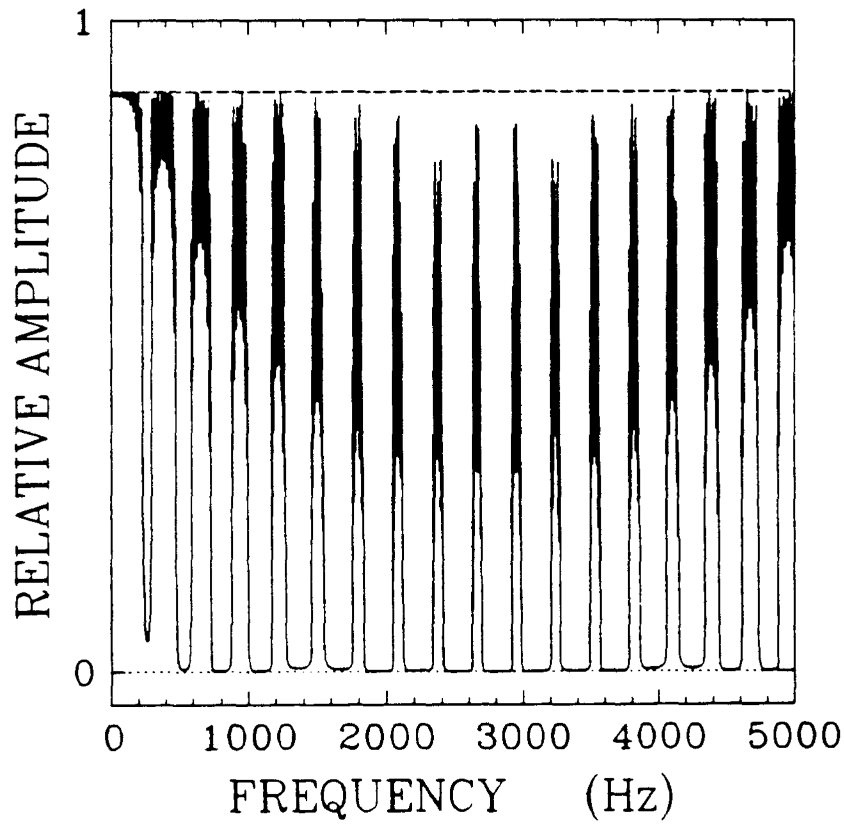

Figure 6: Frequency Spectrum of Impulse Response. (The dashed line represents the input pulse.)

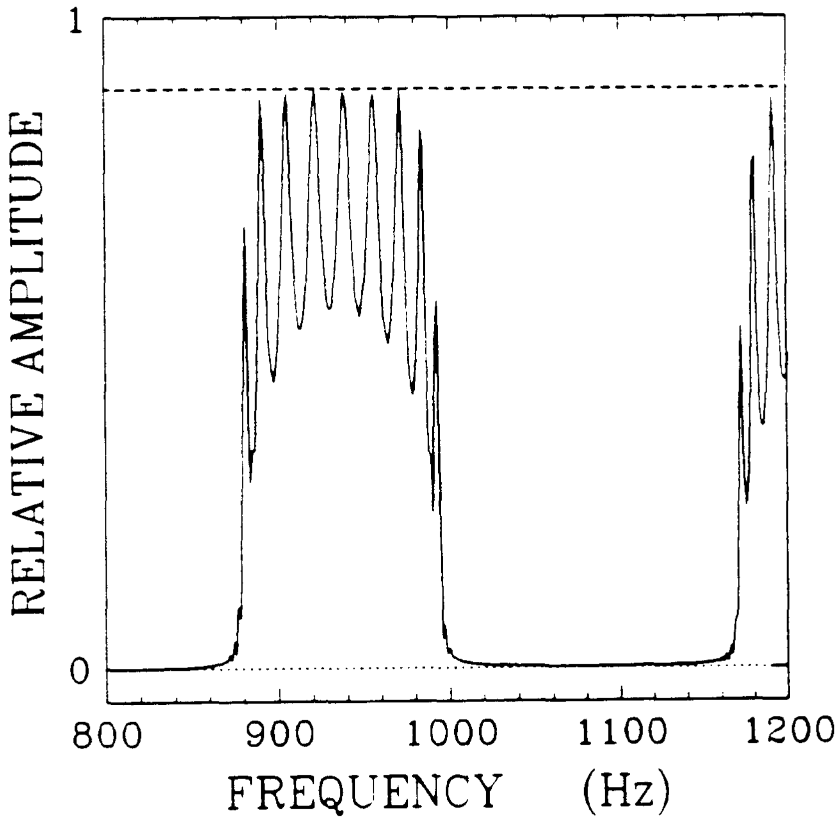

Figure 7: Frequency Spectrum of Fourth Passband of Impulse Response.

In comparison, frequencies in the passbands have propagated with little reduction in amplitude.

Intuitively, Figure 6 should contain sharp jumps at the edges of the passbands and no attenuation within these bands. It does not, partly because of the limited sampling time used for the Fourier transform, about 0.72 s. Figure 2 shows that near the edges of the passbands, the group velocity drops to zero. Therefore some of the energy of the impulse cannot reach the right boundary during the sampling time.

Another cause of this structure is the finite length of drill string. Figure 7 shows an expanded view of the fourth passband in Figure 6. A fine structure similar to that reported in [2] is evident as a series of spikes spaced about 20 Hz apart. All the passbands have the same number of spikes. This number is related to the number of segments of pipe in the drill string. For example, calculations of strings with 20 segments produce about 20 spikes.

The explanation for this phenomenon is simple. The width of each passband is determined by the frequency change required to fit an additional half wavelength into each segment. Thus in a drill string with ten tool joints and 9 pipes, there are 9

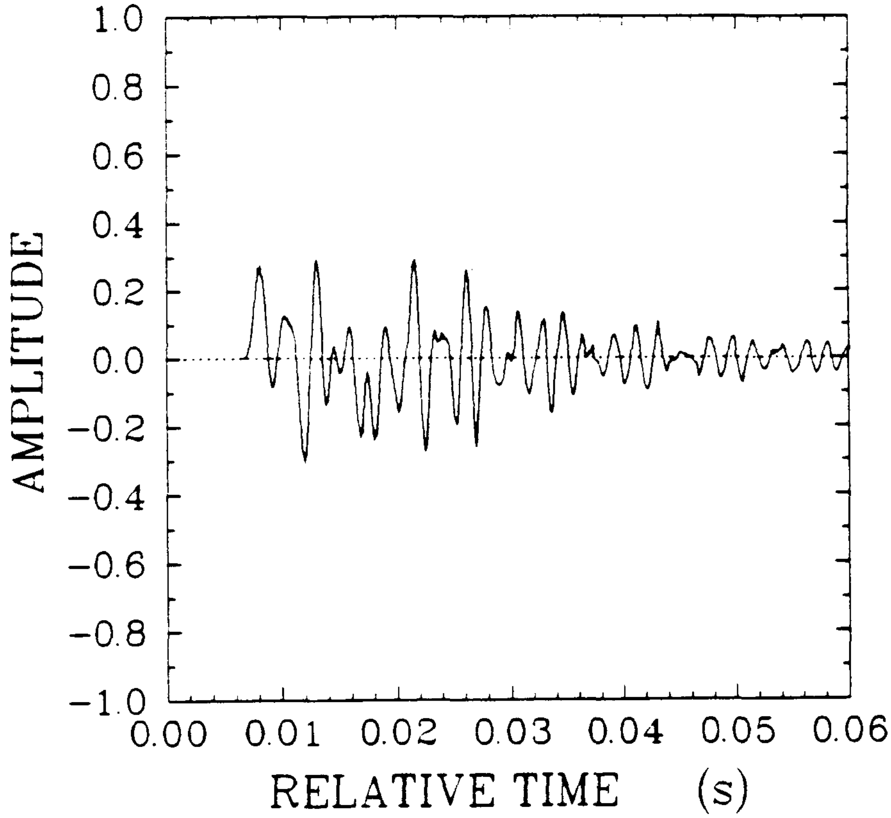

Figure 8: Transmitted Wave Through 9 Segments—5 Sinusoidal Pulses at 525 Hz.

frequencies within the interior of each passband for which an integer number of half wavelengths will fit into the total length of the string. A resonance occurs at each of these frequencies and manifests itself as an individual spike in Figure 7.

In past efforts to use the drill string as a data transmission line, bursts of sinusoidal waves have been used to transmit information. For example, a packet of five waves can be used to indicate a one in a sequence of data bits. Consequently, it is informative to examine the behavior of this type of wave packet. Figure 8 contains a plot of the transmitted wave profile produced by five sinusoidal waves of unit amplitude and frequency of 525 Hz. As with the impulse results, the transmitted wave bears no resemblance to the input wave. The oscillations are greatly reduced in amplitude and continue for a long period of time. By referring back to Figure 2, it is noted that the dominant frequency of this wave packet is located in the center of the second stopband. Consequently, the source of this drastic change in the form of the wave is easily understood. Figure 9 shows a comparison of the frequency spectra of the input and transmitted waves. They differ significantly in that the stopbands have removed groups of frequencies from the wave. What is not illustrated by Figure 9 is that the

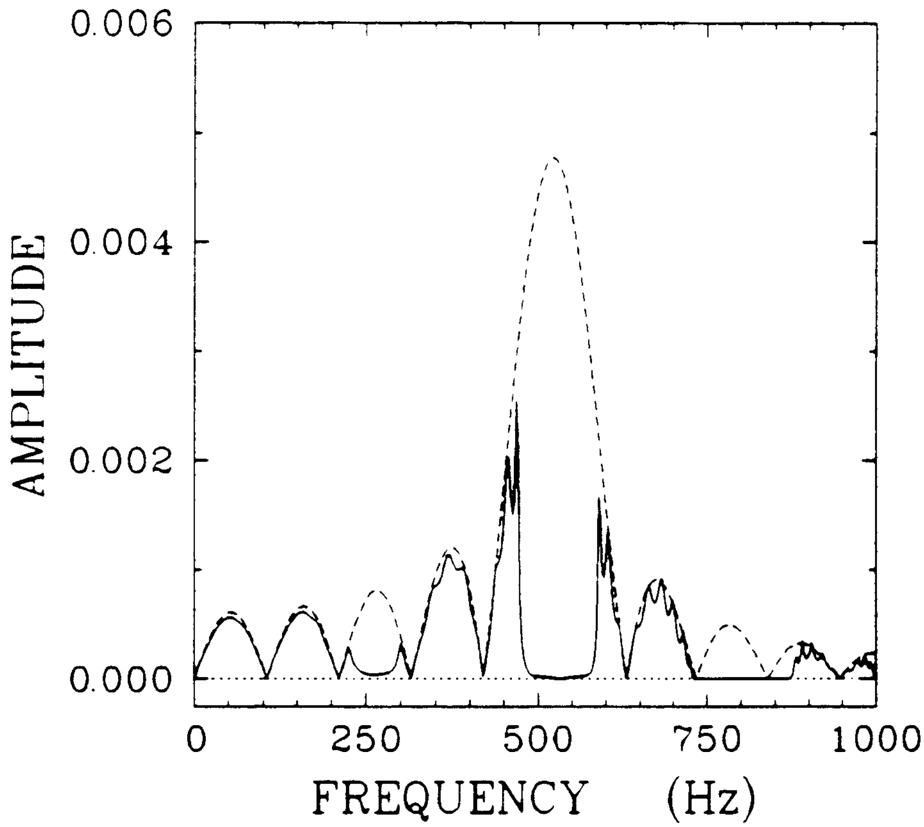

Figure 9: Initial (Dashed Line) and Transmitted (Solid Line) Frequency Spectra from Figure 8.

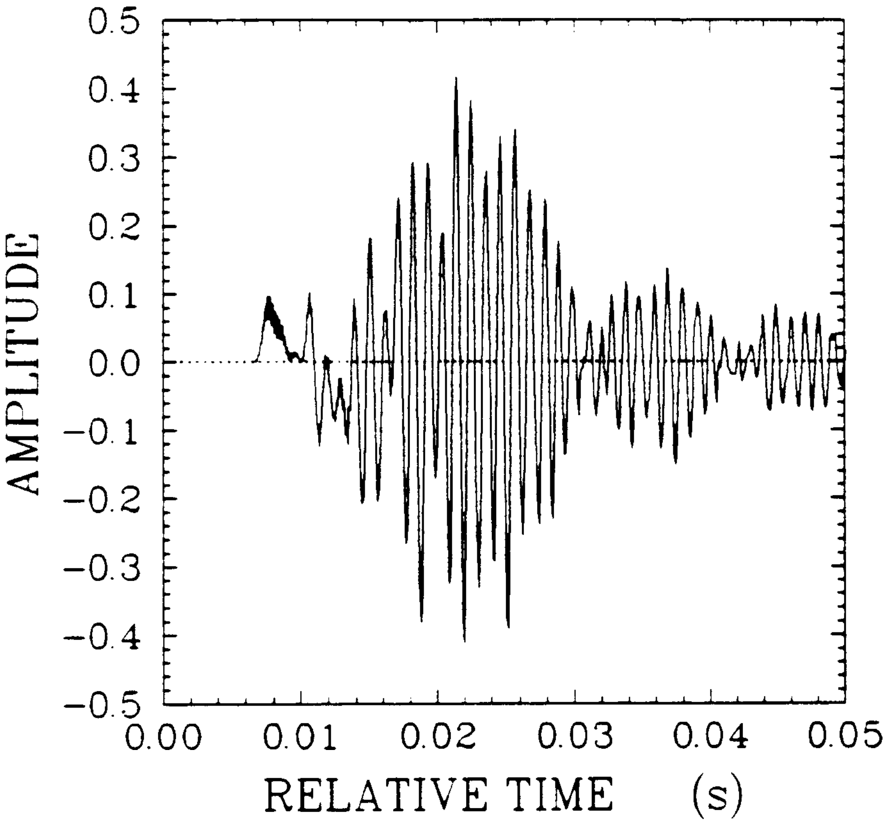

Figure 10: Transmitted Wave Through 9 Segments—5 Sinusoidal Pulses at 960 Hz.

remaining frequencies have also been dispersed due to the curvature of the dispersion curves.

Figures 10 and 11 contain plots of the transmitted wave and a comparison of the input and transmitted frequency spectra for a packet of five oscillations of 960 Hz frequency. In the Cox and Chaney patent [1], this is considered to be an optimum transmission frequency. It falls in the middle of the fourth passband. Again it is observed that the input spectrum has frequencies which overlap into the adjacent stop-bands. The transmitted signal is heavily attenuated and dispersed. These problems can be partially overcome by using a narrower input spectrum. This is achieved by increasing the number of pulses in the input wave from five to ten. Figures 12 and 13 contain the results for this case. Most of the dominant lobe of the input spectrum is present in the transmitted wave; however, due to dispersion within the passbands, the transmitted wave is still distorted. The peak amplitude of the transmitted wave is the best of all the cases illustrated so far, but the form of the wave does not indicate that it originally came from a signal with ten pulses.

Figure 13 also exhibits the fine structure discussed earlier. As before 9 spikes are

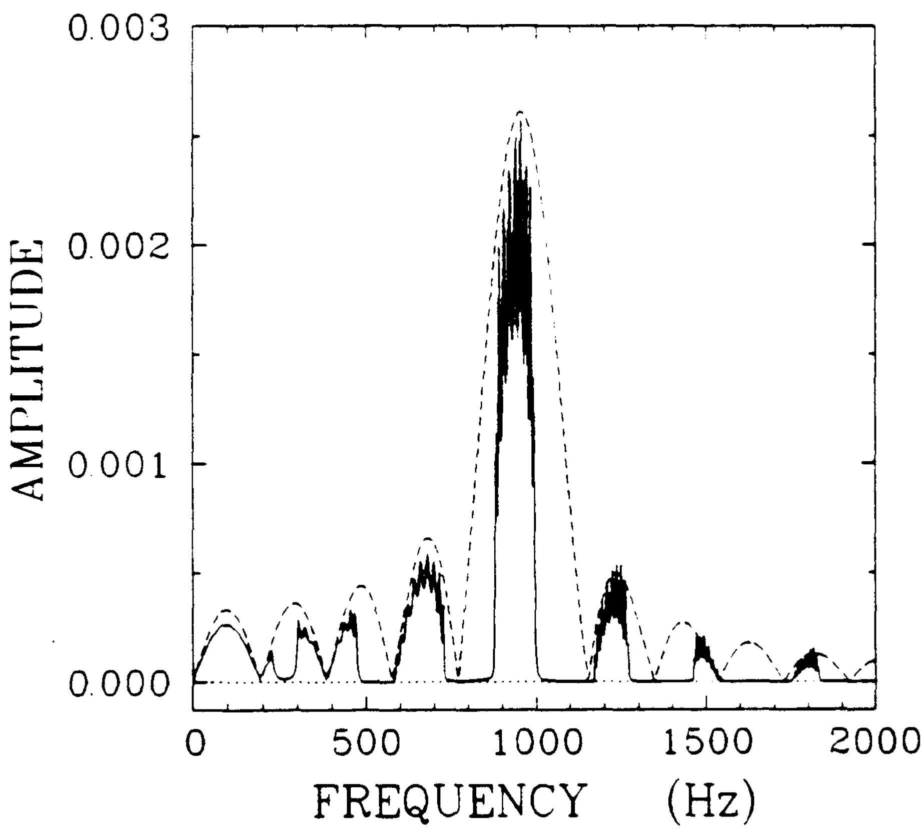

Figure 11: Initial (Dashed Line) and Transmitted (Solid Line) Frequency Spectra from Figure 10.

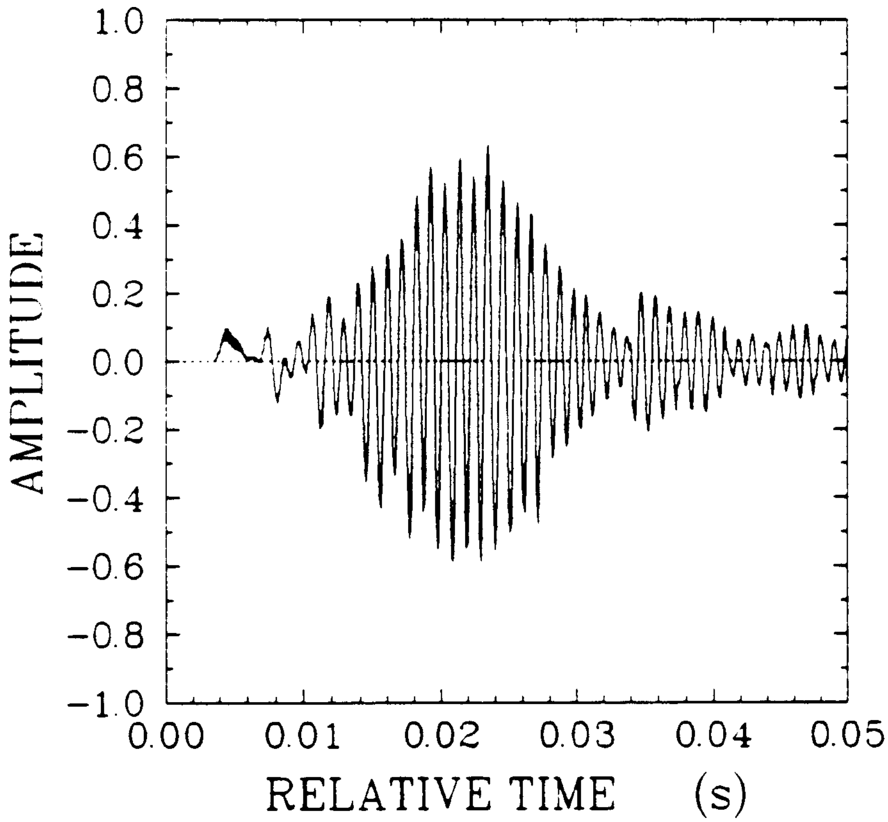

Figure 12: Transmitted Wave Through 9 Segments—10 Sinusoidal Pulses at 960 Hz.

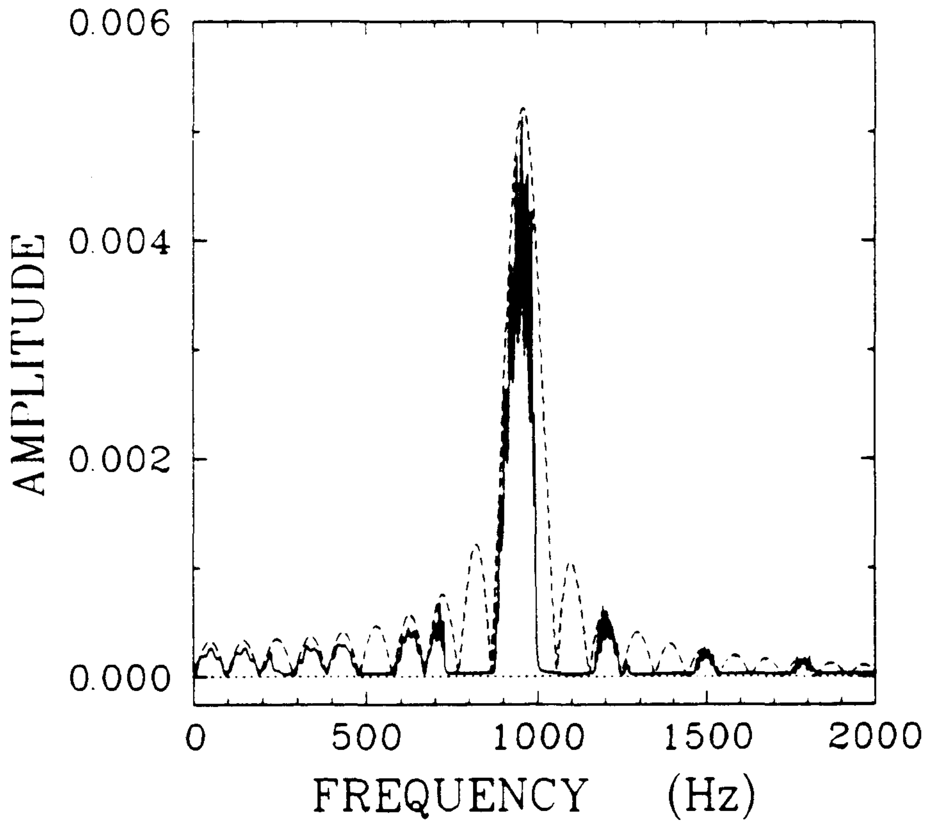

Figure 13: Initial (Dashed Line) and Transmitted (Solid Line) Frequency Spectra from Figure 12.

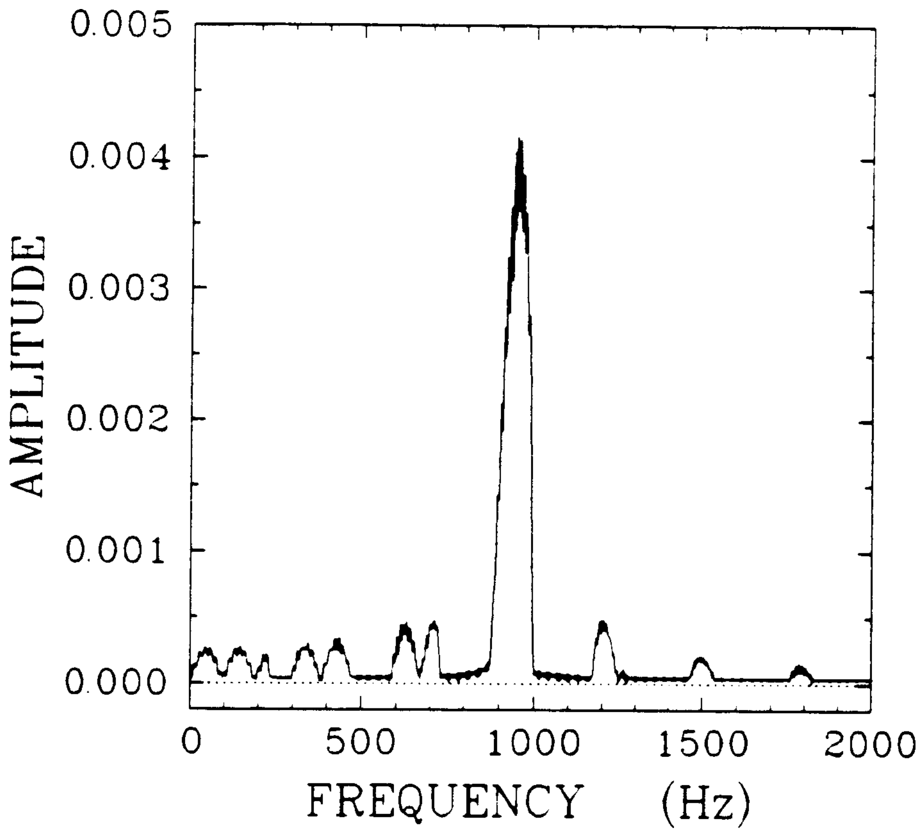

Figure 14: Transmitted Frequency Sprectrum Through 19 Segments—10 Sinusoidal Pulses at 960 Hz.

present in the dominant lobe. The results for transmission through 19 and 39 lengths of pipe are shown in Figures 14 and 15. For 39 lengths of pipe, the spikes are so numerous and small in amplitude that they virtually disappear. Their disappearance from the spectra for the longer strings is due to the fixed sampling time used for the Fourier transform. The spikes result from resonance effects produced by echos across the entire length of the drill string. Longer strings have longer echo times. Thus with a fixed sampling time, less energy from the echos is included in the samples of the longer strings.

Interpretation of experimental results can be confused by these phenomena. For example, a simple comparison of the relative amplitudes of the dominant frequencies in Figures 13 and 14 indicates an apparent attenuation in the signal energy of 4.6 dB/1000 ft. The implication of this result might be that every 1000 feet of the drill string produces an additional 4.6 dB of energy loss. However, this is not the case. In these calculations there is no physical dissipation mechanism, and hence there is no attenuation. Only distortion exists, and as Figures 14 and 15 show, this decreases

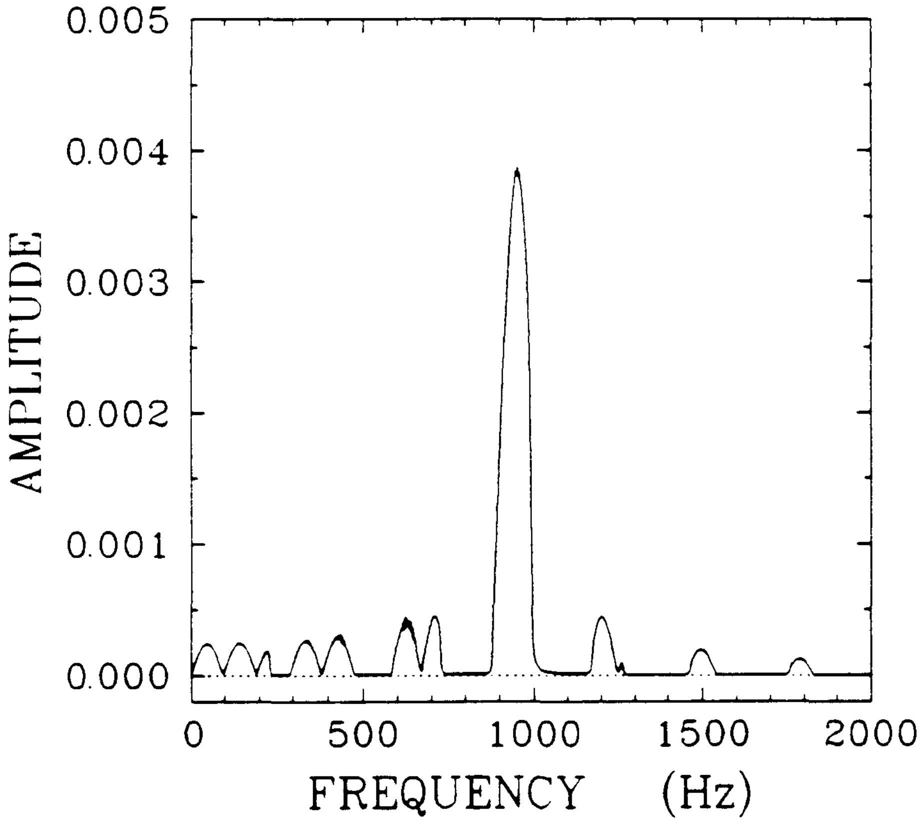

Figure 15: Transmitted Frequency Sprectrum Through 39 Segments—10 Sinusoidal Pulses at 960 Hz.

dramatically with propagation distance.

These examples suggest a method for processing data signals and compensating for the effects of the stopbands and dispersion. The method is simple. First, transmit information only in the passbands and away from the edges of the stopbands. Second, compensate for dispersion by multiplying each frequency component by $\exp(-ikL)$, where L is the transmission length. When a large amount of ambient nose is present, it is best to transform the signal before transmission. This results in an undispersed signal at the receiver position which is more easily recognized.

The input signal shown in Figure 9 is used to illustrate this method. From a practical point of view, due to the broad frequency range of the signal, this is an extreme case. To transmit the data, each frequency component in Figure 9 is shifted to a different frequency which falls in a passband of the drill string. This allows all of the data frequencies shown in Figure 9 to be transmitted on carrier frequencies which are not blocked. After transmission, the carrier frequencies are shifted back to the original data frequencies.

For this example, only carrier frequencies with group velocities greater than 70 percent of the maximum group velocity within each of the first sixteen passbands are used. This frequency-shifted signal is then transformed by the factor $\exp(-ikL)$ and used as a displacement boundary condition to drive the first segment in the drill string.[4] Figure 16 illustrates this wave after it has propagated through ten lengths of pipe. In comparison to Figure 8, the signal is much stronger and less dispersed. If the carrier frequencies of this signal are now shifted back to their original positions in the data spectrum, the inverse transform of the resulting spectrum gives Figure 17. The five pulses of the original signal are clearly evident. Furthermore, the calculations show that the amplitude and form of this wave do not change when transmitted through much longer drill strings.

3 EXPERIMENT

Section 2 presents a detailed theoretical analysis of the acoustical characteristics of the drill string. It is shown that the periodic structure formed by the pipe and tool joint sections results in frequency filtering. A comb filter is produced which exhibits alternating passbands and stopbands. Within each passband significant phase distortion is present. The effects of standing waves produced by multiple echos between opposite ends of a finite-length drill string also manifest themselves through numerous spikes within each of the passbands of the transmission spectrum. The results of this analysis illustrate the importance of suppressing echos and compensating for phase distortion of the signal.

In this section these phenomena are examined through experiment on a 20th-scale

[4]For this calculation, the long section of pipe is removed to insure that the signal produced by the boundary condition enters the drill string.

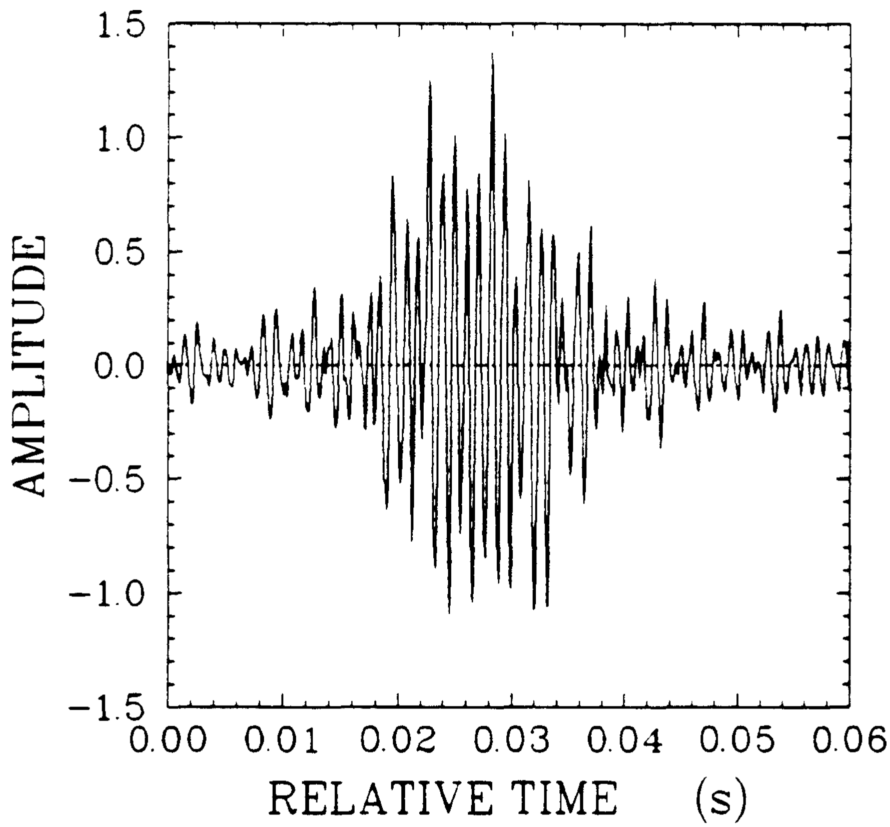

Figure 16: Transmitted Wave for Processed Signal.

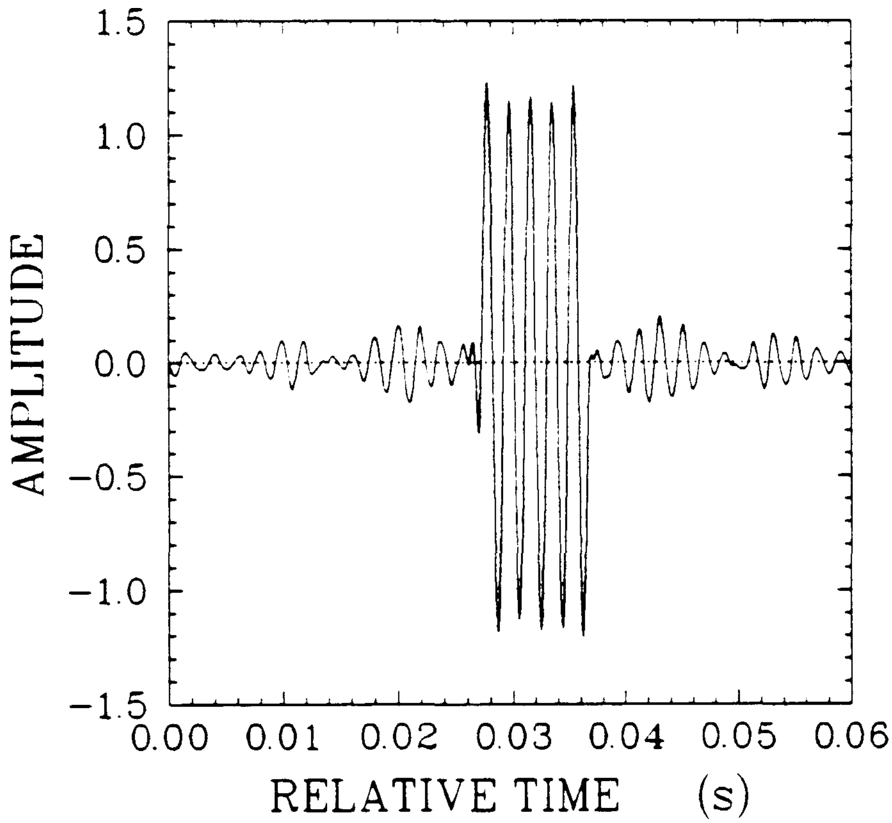

Figure 17: Transmitted Wave after Frequency Shifting.

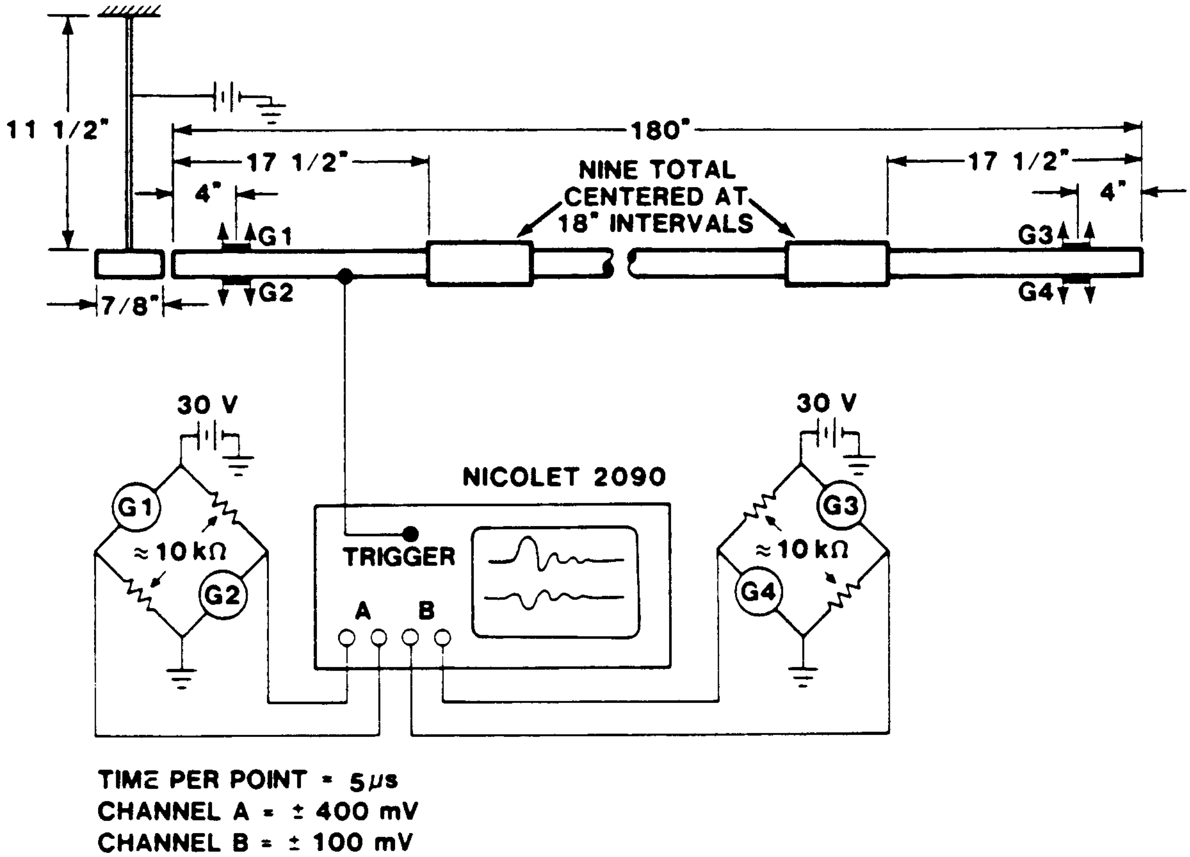

Figure 18: Experimental Apparatus.

model of a drill string. Section 3.1 contains a description of the construction of the model and the experimental apparatus which is used to test the impulse response of this model. Section 3.2 describes the results and compares them to calculations obtained from the theory developed in Section 2.

3.1 The Apparatus

The experimental apparatus is illustrated in Figure 18. The model of the drill string is shown at the top of this drawing. It consists of a 15-ft section of hardened, $\frac{1}{4}$-in diameter, copper water pipe. Nine copper collars are soldered at 18-in intervals along the length of this pipe. The dimensions of these elements are listed in Table 2. This model approximates to 20th scale a nominal $4\frac{1}{2}$-in, 16.6-lbs/ft, American Petroleum Institute drill pipe [9]. Centered at 4 in from each end of the scale model are two sets of strain gages. They are semiconductor gages, Type S/AHP-10,000-300, manufactured by Kulite Semiconductor Products, Inc. They have a nominal resistance of 10,000 Ω, an active gage length of 0.3 in, and a gage factor of 175. The actual resistance of

Table 2: Model Parameters

parameter	pipe	collar
outside diameter	0.252 *in*	0.404 *in*
inside diameter	0.200 *in*	0.252 *in*
length of section	17 *in*	1 *in*

the gages varies about ±10% of the nominal value; however, the gages are paired so that the variation within a set is within ±5%. The mounted gages are calibrated by applying a bending moment to the scale model at each location and measuring the resistance change of each individual gage with a completion bridge. Within a gage pair the relative calibration is within 2%; however, the sensitivity of the gages at the left location is 1.26 times the sensitivity of the gages at the right location.

An impulse load is imparted to this scale model at the left end using a short length of the copper water pipe attached to a slender cantilever beam, a $\frac{1}{16}$-in spring steel wire. When this hammer is drawn back approximately one inch and released, impact activates the external trigger of the oscilloscope by means of the circuit shown in Figure 18. The resulting stress wave is approximately 60 μs in duration and on the order of 1500 lbs/in^2 in amplitude. After impact, the hammer separates, resulting in a stress-free boundary at the left end of the scale model.

This disturbance is measured at each gage location. As shown in Figure 18, each set of gages are connected to a completion bridge. By connecting the gages to opposite sides of the bridge and balancing the bridges so that each gage is subject to an equal voltage, the output signal of each bridge is sensitive to the average axial strain and insensitive to bending motion. The bridge is driven by a 30-v power supply, and the output is connected to a Nicolet digitizing oscilloscope, Model 2090. This device can digitize and store 4000 data points per channel. The data is digitized at a rate of one point per 5 μs which corresponds to a total recording time of 20 ms. The nominal calibration of the bridges is 381 microstrains per volt; however, the measured calibrations using the method described above are 273 microstrains per volt for the left gages, and 344 microstrains per volt for the right gages.

Immediately after impact, the left set of gages record the resulting right-traveling wave. The wave reflected from the first collar does not return to this gage location until more than 200 μs have elapsed. A typical record of this initial wave is shown in Figure 19 which is a plot of voltage versus time after impact. Only the digitized data points are plotted. Ideally, this plot should contain a square wave of approximately 12 μs duration [8]. The actual duration is much larger due to misalignment of the hammer and curvature of the impact surfaces. These errors also produce bending waves in the scale model. The axial strains resulting from these bending waves are measured to be less than 10% of the amplitude of the maximum longitudinal motion.

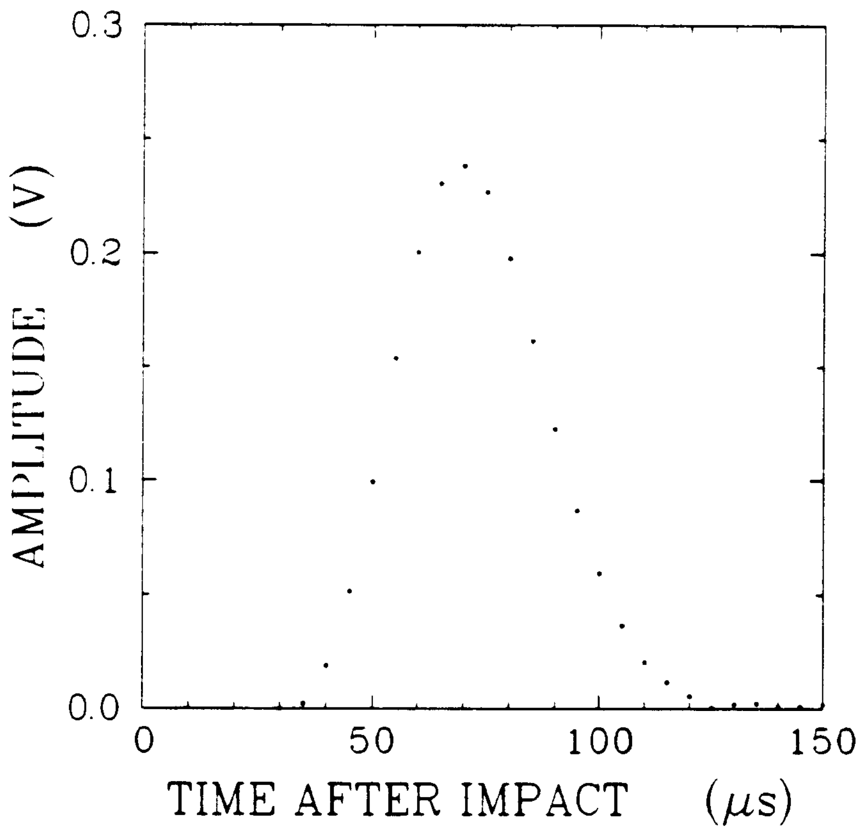

Figure 19: Initial Wave Resulting from Impact.

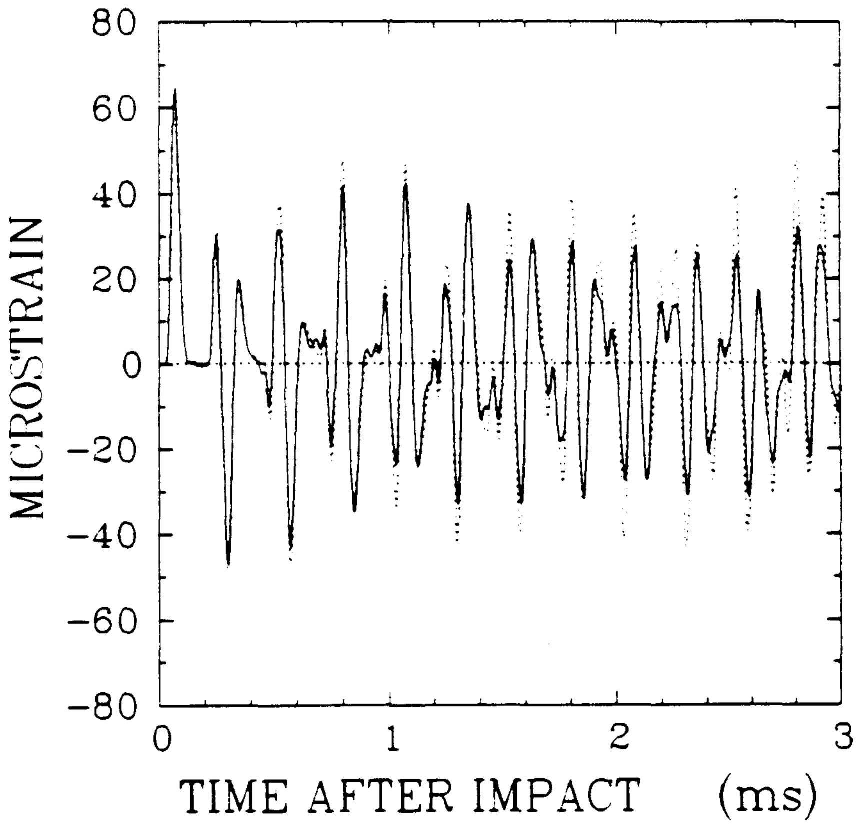

Figure 20: Time-History at the Left Gage Location. (The solid lines are data and the dotted lines are calculation.)

Because of the relative position of the two gages at each location, bending motion produces equal and opposite strains in each gage and results in self-canceling voltages in the completion circuit.

The solid lines in Figures 20 and 21 represent a typical time history collected at both the left and right gage locations. The dotted lines represent the calculated results. They will be discussed in the next section. Axial strain is plotted against time after impact. On this scale of time, the numerous reflections from each of the collars can be seen. The effects of reflections from free surfaces at both ends of the scale model are also present.

By looking in detail at Figure 20, the first positive pulse can be identified as the initial wave resulting from the impact. This is the wave shown in Figure 19. The next positive pulse is the left-traveling wave reflected from the first collar. This is followed immediately by a negative right-traveling wave which is a reflection from the free surface at the impact boundary.

The time delay before arrival of the first wave in Figure 21 is due to the travel time

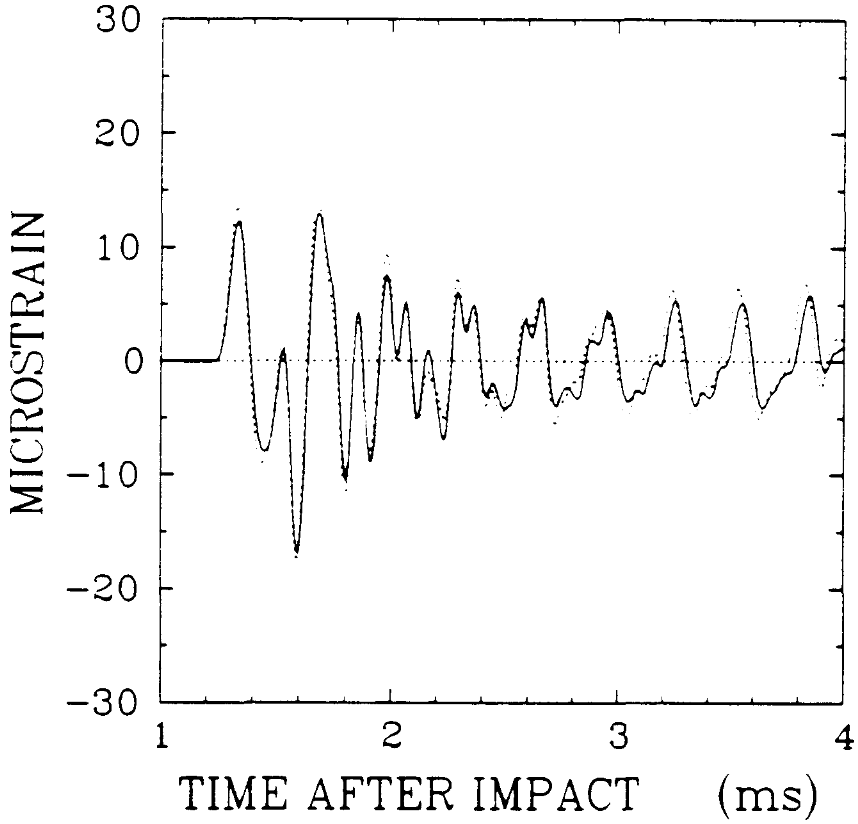

Figure 21: Time-History at the Right Gage Location. (The solid lines are data and the dotted lines are calculation.)

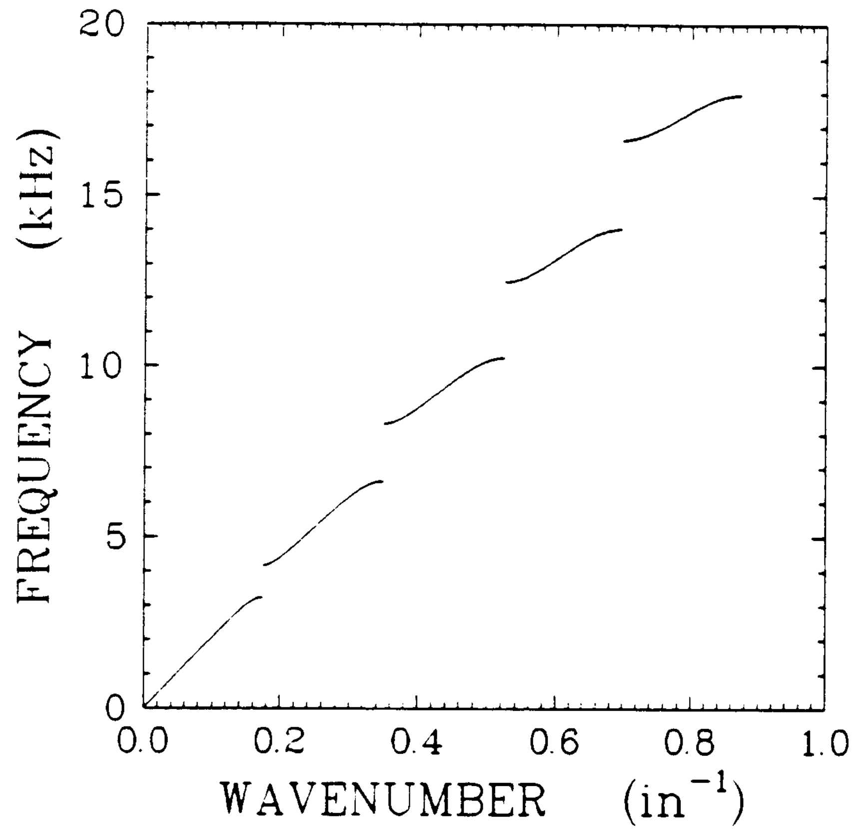

Figure 22: Calculated Dispersion Curves for the Scale Model.

along the length of the scale model. It is obvious through comparisons of these two figures that the data in Figure 21 contains significantly lower frequencies than the data in Figure 20. The scale model has acted as a frequency filter.

3.2 Results

The analysis presented in Section 2 of this work can be used to calculate the response of both time-harmonic and transient waves. Figure 22 contains the dispersion curves for the scale model. These calculations are obtained using a specific gravity for copper of 8.96 and a bar velocity of 143,000 in/s.[5]

These dispersion curves illustrate why the high frequencies are trapped at the impact

[5]The apparatus described in the last section was used to measure the wave velocity in a 14-ft length of copper water pipe. A value between 143,000 and 144,000 in/s was measured. This is slightly lower than the nominal value of 148,000 in/s for pure, oxygen-free copper. Since only trace elements are present in the copper used to manufacture this pipe, the discrepancy is believed to be due to the oxides induced during manufacturing.

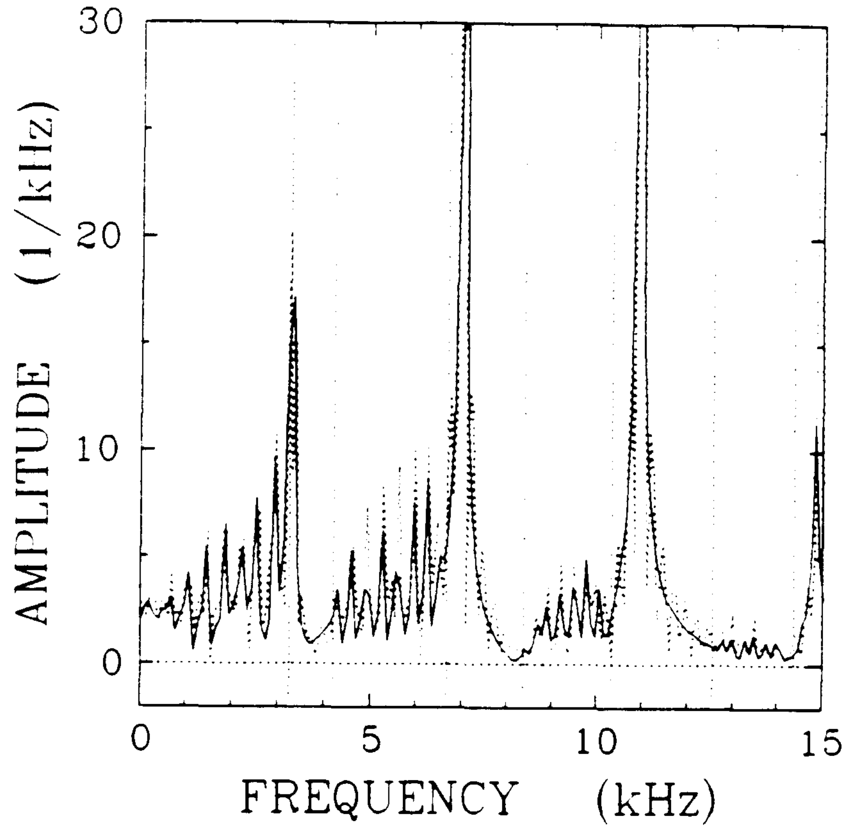

Figure 23: Frequency Spectrum of the Left Gage Location. (The solid lines are data and the dotted lines are calculation.)

location on the left end of the scale model. As discussed in Section 2, these curves map the passbands, and the stopbands are indicated by the gaps between the curves. As the frequency increases, the width of the stopbands increases indicating that more of these frequencies are blocked by the filtering effect of the periodic structure. This is verified by performing a Fourier transform of the 16 ms of time-history data. Figures 23 and 24 contain the results. The dotted curves in these plots are theoretical results which will be discussed shortly. The vertical dotted lines are the predicted boundaries of the passbands shown in Figure 22. Figure 23 which contains the results for the left gage location, shows large amounts of energy contained within the stopbands. These frequencies have been trapped at the impact end of the scale model. Figure 24 shows that at the opposite end from the impact, significant amounts of energy reside mostly within the passbands.

Within each passband the data exhibit a regular pattern of spikes. As discussed in Sections 2 and 3, this pattern is attributable to a standing-wave effect produced by repeated echos between the left and right boundaries of the scale model. The number

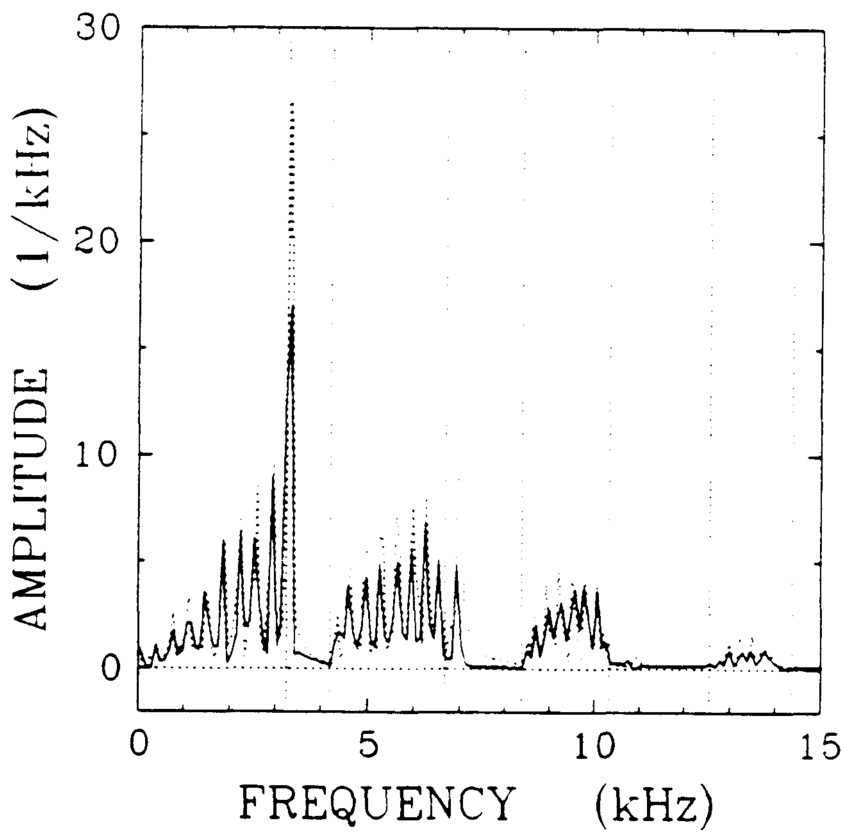

Figure 24: Frequency Spectrum of the Right Gage Location. (The solid lines are data and the dotted lines are calculation.)

of spikes in each passband correlates to the number of collars on the scale model.

This experiment can also be modelled using the transient wave analysis contained in Section 2. The first 170 μs of the initial wave resulting from the hammer blow, see Figure 19, can be used as the left boundary condition for the calculation. For later times this boundary is assumed to be stress free. The mesh size used for this calculation is 0.25 in. The time-histories resulting from this calculation as well as the Fourier transform of these histories are shown as dotted lines in Figures 20, 21, 23, and 24.

In Figure 20 the error between the calculation and the data is primarily in the over prediction of the pulse amplitudes. However, the overall agreement with the data is quite good, and most of the fine detail of the late-time wave profile is accurately represented in the calculation.

In Figure 21 the comparison is even better. Exceptionally fine detail is accurately represented by the calculation. It is again noted that no shifting or rescaling of the data or calculation has been used. Both the times and amplitudes are recorded as measured and as calculated.

The Fourier transforms of the calculated waves are shown in Figures 23 and 24. The pattern of spikes match well in frequency. The major discrepancies between the amplitude of the calculated spectrum and the data occurs both in the second passband at about 6 kHz and in the third stopband at about 11 kHz. The 11-kHz discrepancy correlates with the over-calculated amplitudes in Figure 20.

4 FIELD TEST

Sections 2 and 3 contain results from both theoretical analysis and laboratory experiment on an idealized model of a drill string. The results of that work show the relationship of the telemetry problem to the classical Brillouin wave scattering problem [5]. The system exhibits a transmission spectrum which has passbands and stopbands. Within each passband, wave dispersion is present but attenuation is very low or absent. These phenomena result from the resonance effects between neighboring tool joints. The finite length of the drill string also produces resonances. When these finite-length effects are superimposed on the Brillouin scattering response, a complex spike pattern or *fine structure* appears in the frequency spectrum of each passband.

All of these phenomena are predicted by analysis of an idealized system in which wave absorption is ignored. The actual system is composed of drill pipe with low dimensional tolerances, tool joints with complex geometry, and drill string assemblies which are submerged in drilling mud. Ultimately, the effects of these irregular structures and sources of attenuation can only be judged through a field test. It is the purpose of this section to examine the magnitude of these effects and the relevance of the idealized system in predicting the response of the field system.

Section 4.1 contains a description of a field test performed by **Sun Oil Company** in 1975. The analog data collected from this test are digitized and analyzed by a method described in Section 4.2. In Section 4.3, comparisons are made to the theory developed in Section 2 and to the laboratory experiment reported in Section 3.

4.1 The Field Test

Cox and Chaney [1] describe a field test which was performed by Sun Oil Company in July, 1975. It was the basis for their patent on an acoustical telemetry system. The description of the field test and the format in which the results were presented were incomplete. However, discussions with Preston Chaney provided additional information about the field test and the original data tape.

Some information about the test is still missing, and the design of the test precludes a careful quantitative analysis of the data. In spite of these deficiencies, the results provide important and unique information concerning the behavior of acoustic waves in a drill string submerged in a well filled with drilling mud.

The test was designed to examine the frequency response of a drill string constructed of $4\frac{1}{2}$-in drill pipe with a nominal weight of 16.6 lbs/ft. The type of tool joints used on this string are unknown. They were either API regular or API full hole [9]. Both types are of the same length and have approximately the same cross-sectional area. The total length of each section of pipe with tool joints was 31.3 ft. This string was suspended in a relatively straight well which was filled with drilling mud. An acoustic pulse was generated by screwing a steel cap onto the top of the string and striking it with a ball peen hammer. The signal which traveled the length of the drill string was measured by a transducer described only as a "conventional crystal accelerometer" [1]. The analog signal produced by the accelerometer was recorded on a cassette tape. The accelerometer, tape recorder and power supply were placed within a sealed chamber which was mounted to the bottom of the drill string. Signals were measured at five depths; 313, 627,[6] 919, 1253, and 1566 ft. At each depth, the drill string was supported at the drilling rig platform with slips, and ten hammer blows were delivered spaced at intervals of one second.

The acoustical transfer functions of the steel cap, support system, sealed chamber, and accelerometer are unknown. It can only be assumed that they do not change as a function of depth. The boundaries of the passbands within the drill string and the fine structure within each passband can be examined without this information. If it is also assumed that the hammer blows at each depth are identical, comparisons of the data signals for each depth also give information about the evolution of an acoustic wave as it travels along the drill string.

4.2 Data Reduction

The analog data contained on the cassette tape was originally digitized using equipment normally employed for analyzing geophysical data. This equipment had a sampling interval of 2 ms. To accommodate this slow sampling rate, the data tape was dubbed

[6]This depth was incorrectly reported in [1] as 527 ft.

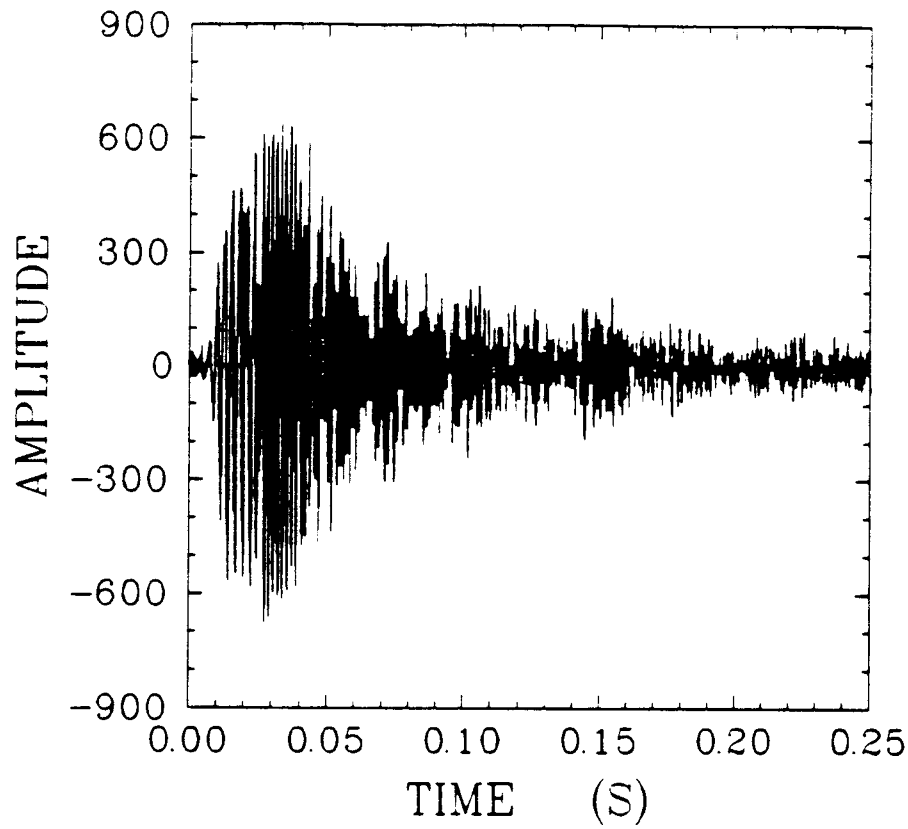

Figure 25: Time History of the 1566-Ft Test.

to another tape for playback at a four-times slower rate. This was repeated again to produce a total factor of sixteen reduction in speed. The final tape was digitized to obtain the results contained in [1].

For the present work, the original tape was digitized at a sampling interval of 50 μs using the data reduction facilities at **Sandia National Laboratories**. This rate corresponded to a Nyquist critical frequency of 10 kHz. At each depth, three one-second records were digitized; a noise sample, the first hammer blow, and the last hammer blow. A string of zeros was then appended to the ends of the data sets containing the hammer blows. These zeros were used to increase the length of each set to $2^{16} = 65,536$ samples.

A Fast Fourier Transform was taken of these data sets. As few as $2^{14} = 16,384$ samples and as many as $2^{16} = 65,536$ samples were used. The only difference between these two transforms was in the refinement in the resolution of the fine structure within each observed passband. The largest number of points resulted in frequency spectra computed at intervals of 0.15 Hz.

Figure 25 is a plot of the digitized signal resulting from the first hammer blow

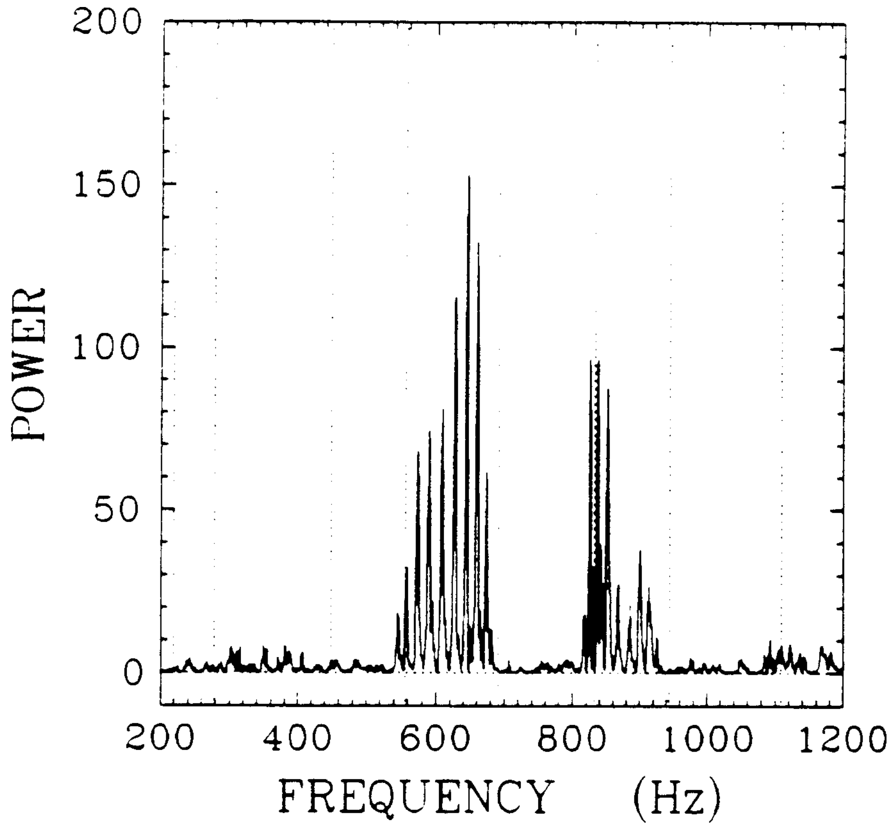

Figure 26: Power Spectral Density of the 313-Ft Test. (The vertical dotted lines indicate the calculated boundaries of the passbands.)

recorded at the 1566-ft depth. Cox and Chaney estimate the duration of the surface signal to be on the order of 1 ms. The signal received by the accelerometer is severely distorted. Even after 0.25 s, ringing is observed which is several times greater then the amplitude of the ambient noise.

4.3 Results

The Fourier transforms of the noise samples show no unusual characteristics. Also, the spectral content of the two digitized hammer blows at each depth are approximately equal. Consequently, only the spectral content of the first hammer blow at each depth is included in these results. Figures 26 through 30 contain the spectra from each of the five depths. These figures are plots of the relative power spectral density versus frequency. At the two shallowest depths, two passbands are clearly evident as a series of sharp spikes, and at the other depths three passbands are evident. These bands are centered at 370, 620, and 870 Hz. Although not shown, no passbands are evident

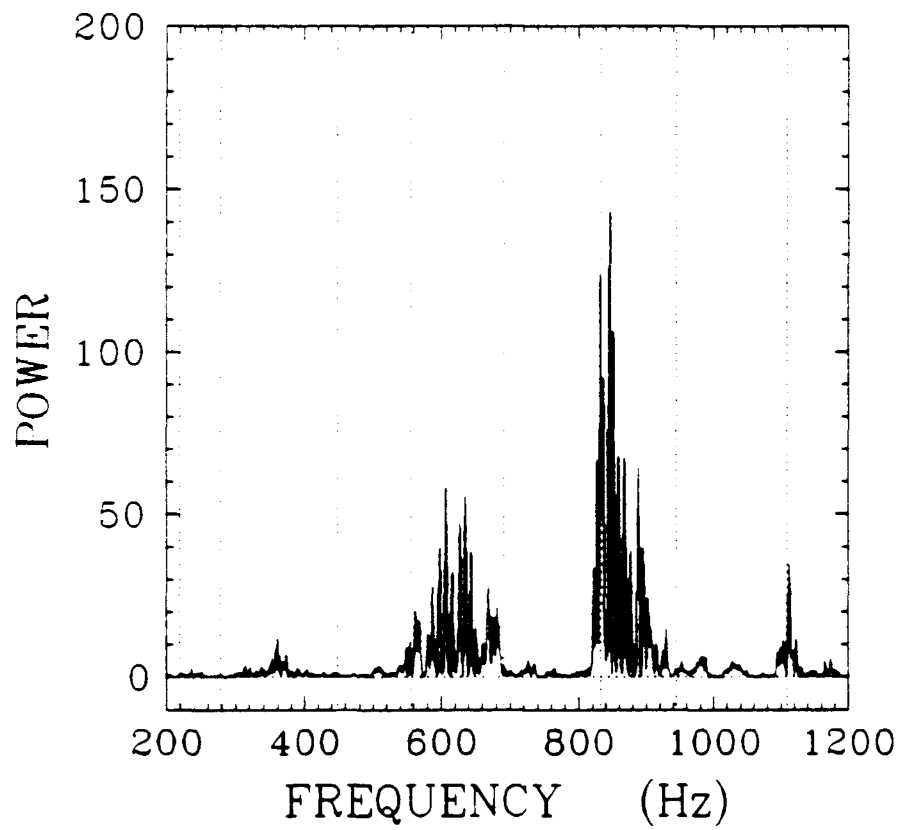

Figure 27: Power Spectral Density of the 627-Ft Test. (The vertical dotted lines indicate the calculated boundaries of the passbands.)

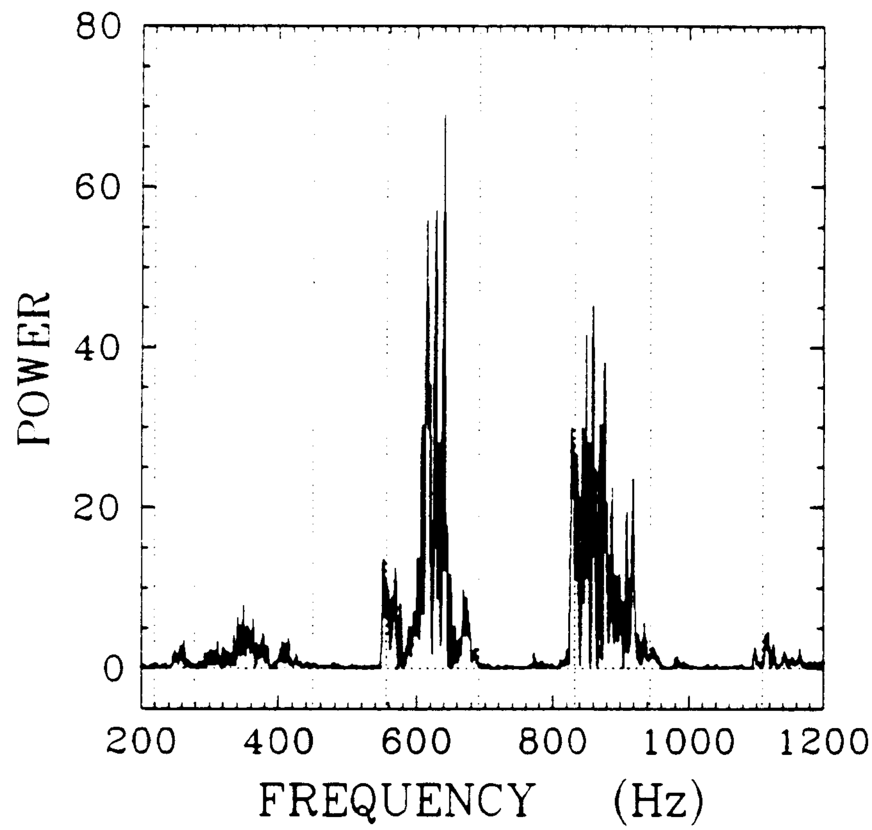

Figure 28: Power Spectral Density of the 919-Ft Test. (The vertical dotted lines indicate the calculated boundaries of the passbands.)

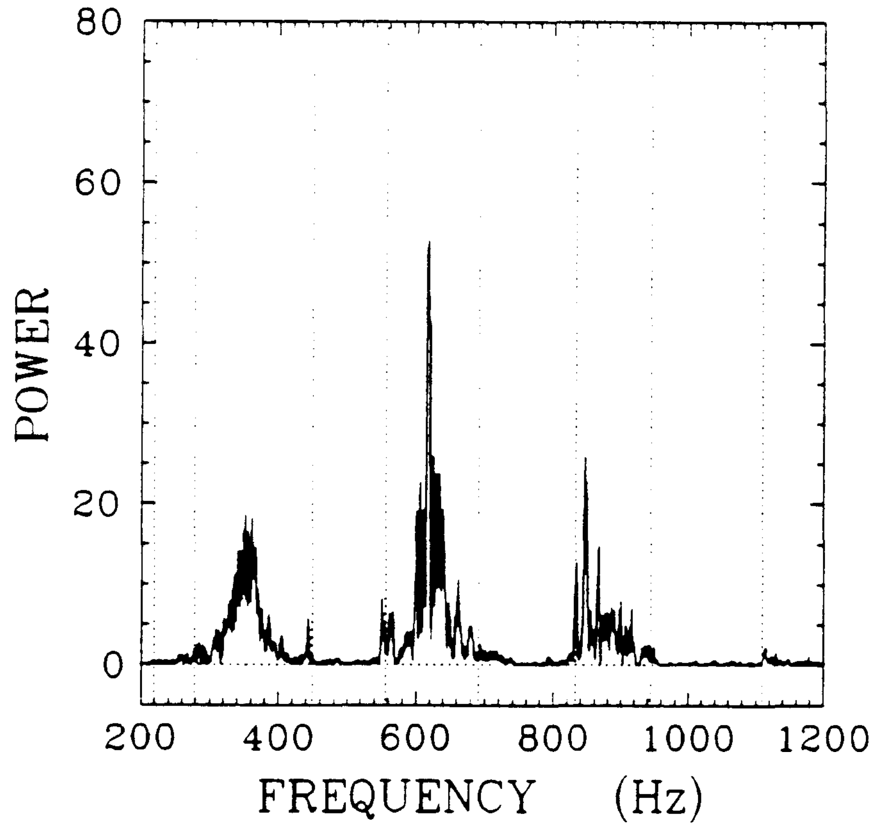

Figure 29: Power Spectral Density of the 1253-Ft Test. (The vertical dotted lines indicate the calculated boundaries of the passbands.)

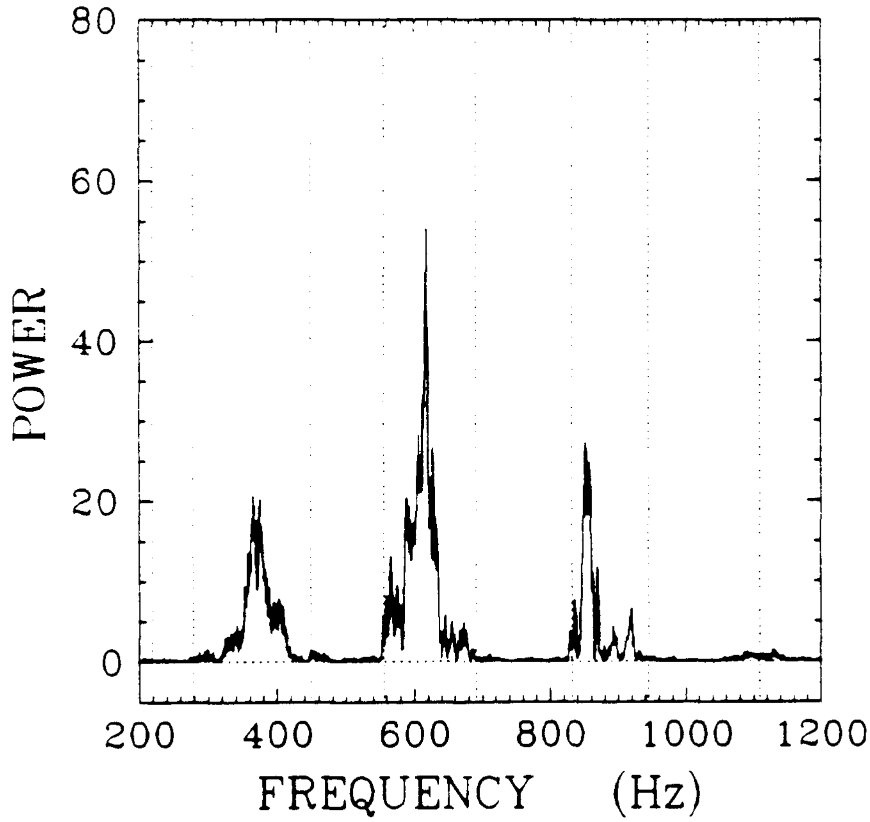

Figure 30: Power Spectral Density of the 1566-Ft Test. (The vertical dotted lines indicate the calculated boundaries of the passbands.)

between 1,200 and 10,000 Hz.[7]

Theoretical estimates of the boundaries of the passbands are also included in these figures. They are illustrated as vertical dotted lines. The method by which these calculations are obtained will be described in Section 4.4. For the present, it is worth noting the good agreement between the theory and the data. In all cases the calculations place the passband slightly higher than the data. The fundamental passband extends from 0 to 219 Hz. The data indicate an absence of energy in this passband.

The absence of any indication in the data of the either the first passband or the fifth and higher passbands is undoubtedly due to the lack of energy in these frequencies as a result of the hammer blow. The reason for the absence of energy in the second passband in the two shallowest records is not apparent. One can only speculate that the increased weight of the longer drill strings may have *tuned* the support structure to the frequencies within this passband or the nature of the hammer blows may have changed.

The data in Figures 26 through 30 are replotted in Figures 31 through 35 on a scale which more clearly illustrates the response in the third passband. The spikes which appear in these data are due to repeated echos bouncing back and forth between the top and bottom of the drill string. As the depth increases, attenuation due to the presence of the drilling mud weakens both the echos and the features which they produce within the passbands.

To illustrate this point, the 1566-ft record, Figures 30 and 35, can be used for an example calculation of the effect of echo suppression. Due to the long length of this drill string, the echos are more clearly separated from the primary signal, and the echo can be suppressed in a crude fashion by simply clipping the trailing portion of the data signal. Based on the bar velocity of steel, the first echo should appear at 0.19 s after the first signal arrival. If the data shown in Figure 25 is replaced by zeros after this point in time, the spectrum shown in Figure 36 is obtained. The spikes are now absent. This process has a similar effect on all the data sets; however, at the shallower depths more of the primary signal is clipped along with the echos.

As discussed in Section 2.4, the lower boundary of each passband corresponds to a frequency where an integer number of half wavelengths fits into each section of the drill string. The high frequency boundary of the same passband has one additional half wavelength in each section. Thus for a drill string with eleven tool joints and ten sections of pipe, ten half wavelengths are introduced into the total length of the drill string as the frequency increases from the lower boundary to the upper boundary of a passband. As each half wavelength is added, a resonance occurs between the ends of the string. Thus the interior of each passband should exhibit ten resonance spikes. Figure 31 illustrates the response of a string with ten pipes. Ten major spikes are

[7]These results differ significantly from those originally published in Cox and Chaney's patent [1]. There the passbands are wider, devoid of spikes, less distinct, and at somewhat higher frequencies. For example, their results place the center of the highest passband at 950 Hz instead of 870 Hz. Unfortunately, the transmission system they propose in their patent makes use of a 940 Hz frequency channel which by the present results falls within a stopband.

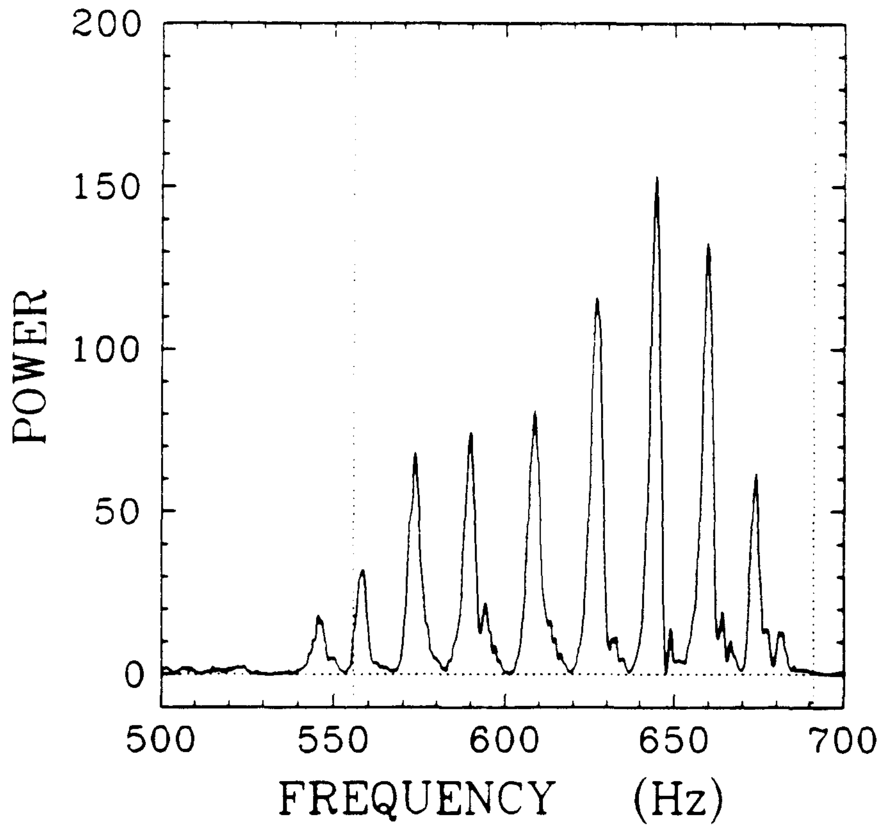

Figure 31: Power Spectral Density of the 313-Ft Test. (The vertical dotted lines indicate the calculated boundaries of the passbands.)

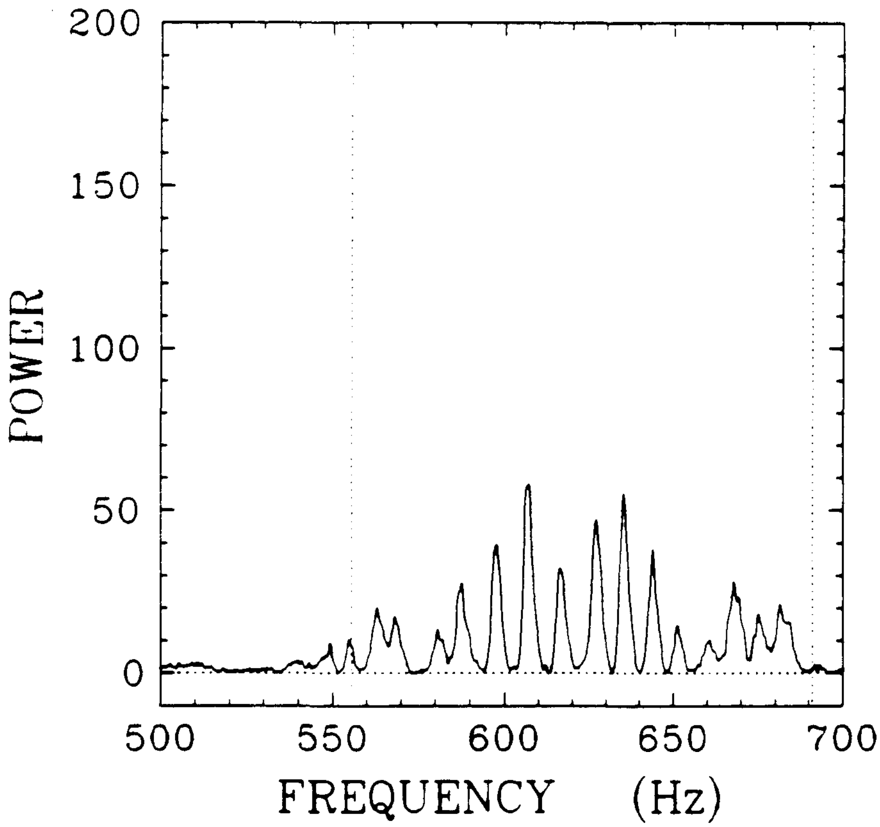

Figure 32: Power Spectral Density of the 627-Ft Test. (The vertical dotted lines indicate the calculated boundaries of the passbands.)

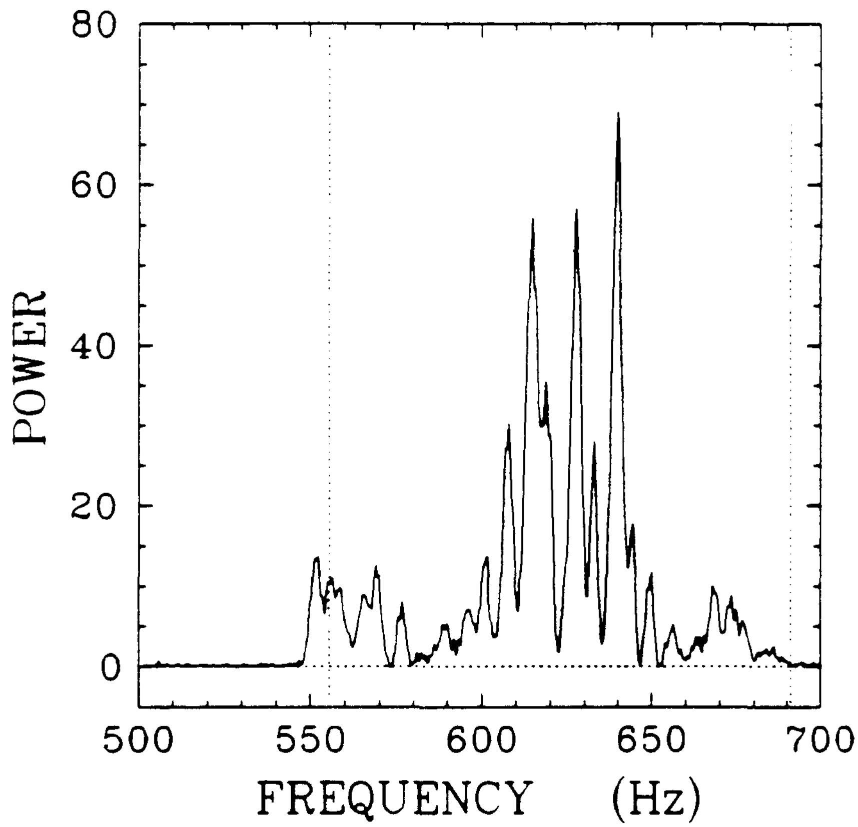

Figure 33: Power Spectral Density of the 919-Ft Test. (The vertical dotted lines indicate the calculated boundaries of the passbands.)

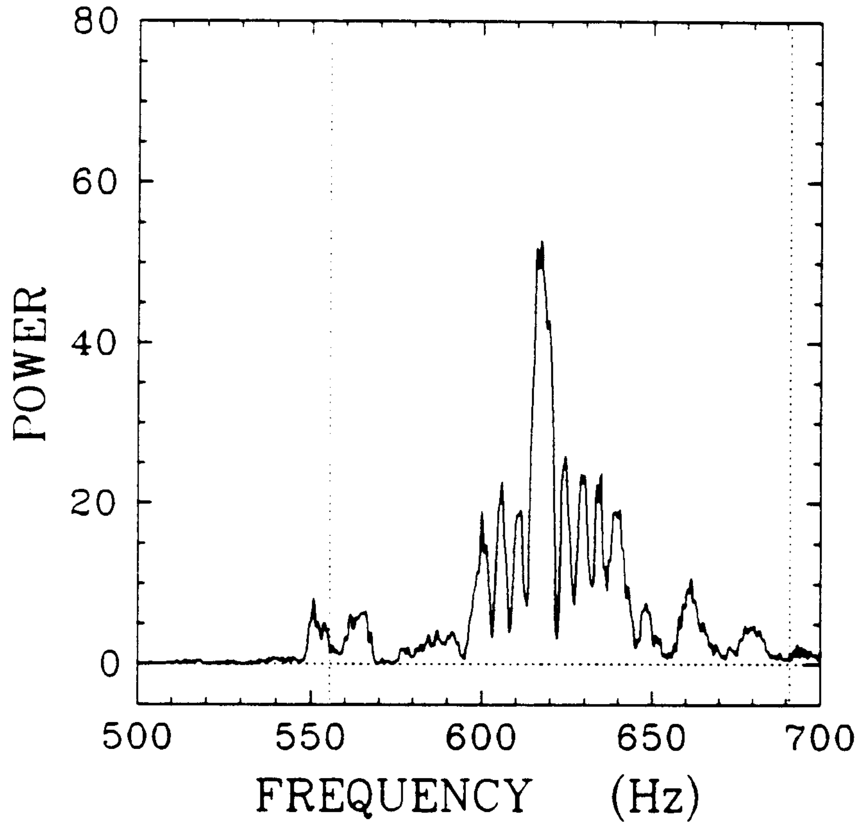

Figure 34: Power Spectral Density of the 1253-Ft Test. (The vertical dotted lines indicate the calculated boundaries of the passbands.)

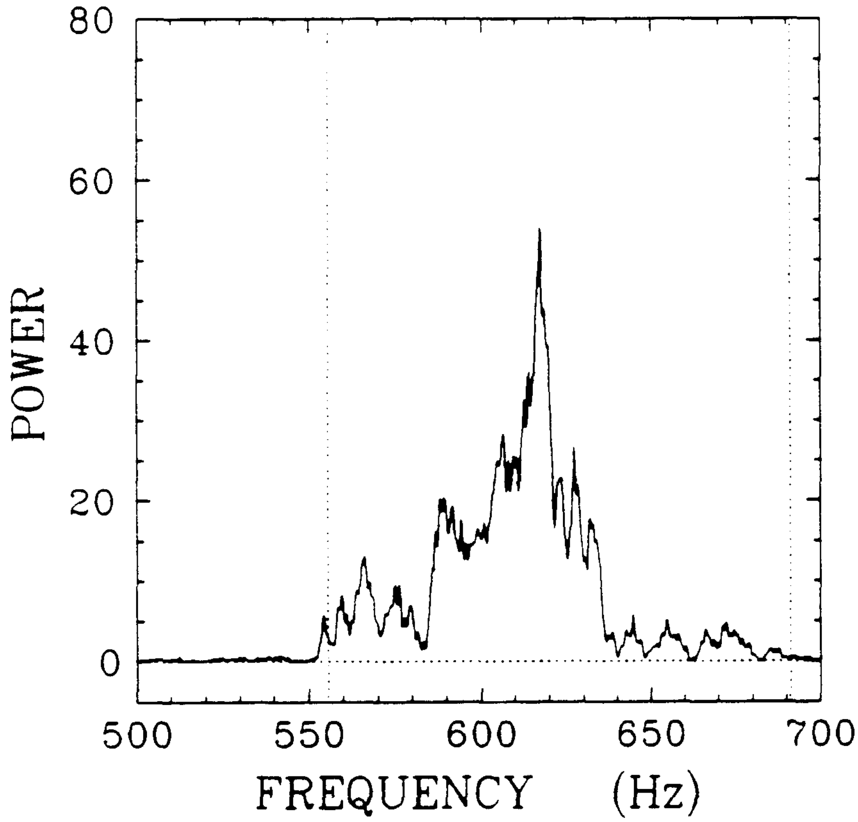

Figure 35: Power Spectral Density of the 1566-Ft Test. (The vertical dotted lines indicate the calculated boundaries of the passbands.)

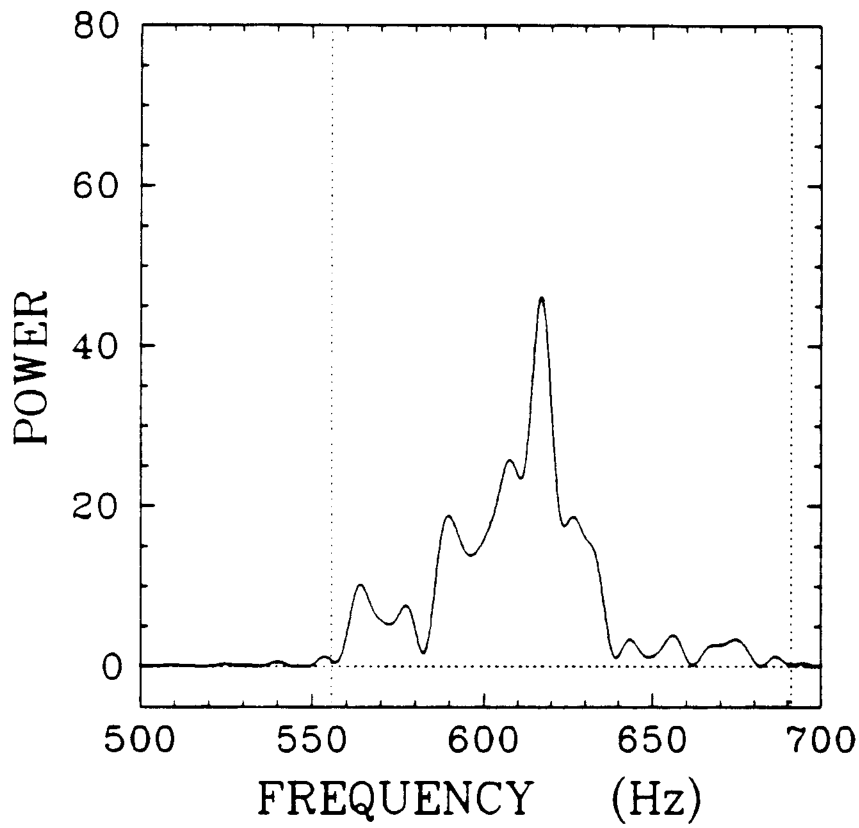

Figure 36: Power Spectral Density of the 1566-Ft Test with Echos Suppressed. (The vertical dotted lines indicate the calculated boundaries of the passbands.)

present in this passband. Minor spikes are also present. The most likely causes of these weaker resonances are the variation in the length of drill pipe sections and irregular wear of the individual tool joints. As much as a one-foot variation is normally allowed in the pipe length, and a 30 percent reduction of cross-sectional area at the tool joints is common.

The spectra of the two passbands at the 313-ft depth each exhibit the same number of spikes. At the 627-ft depth, 20 pipe sections are present. Twenty spikes should be exhibited by the passband shown in Figure 32. In this case about 16 or 17 are present. The imperfections in the structure have a more pronounced effect; however, in this case and the remaining spectra, a strong correlation exists between the number of spikes within each passband and the number of pipe sections within the drill string.

In the record from the deepest test, the existence of the spike pattern indicates that a significant amount of energy traveled three times the length of the drill string or 4700 ft. Comparison of the amplitudes of the 313-ft to the 1566-ft records also gives an estimate of the signal attenuation of 4 dB/1000 ft of propagation. This estimate of attenuation may be high, since this would indicate an echo with a strength of approximately 6 percent of the primary signal at the 1566-ft depth. The spike structure in Figure 35 suggests the echos are about twice that strength.

4.4 Calculations

The theory developed in Section 2 can be compared to the field test results. Since the energy spectra produced by the hammer blows and the transfer functions of various components of the system are unknown, only limited comparisons can be made. The idealized model of the drill string has the following characteristics:

- The cross-sectional area of the pipe is 4.41 in^2.
- The type of tool joint is unknown, but the most probable types all have about the same cross-sectional area. Abrasion of the tool joints may cause larger errors. A value of 19.6 in^2 is used. This value corresponds to a new full-hole tool joint [9].
- The total length of each section is 376 in.
- The length of the tool joint is chosen so that the weight of the actual tool joint equals the weight of the idealized tool joint. The length is 23.5 in.

The eigenvalue analysis in Section 2.2 can be used to determine the response of an infinite drill string to periodic longitudinal acoustic waves. The resulting dispersion curve is shown in Figure 37, and the boundaries of the passbands are shown as vertical dotted lines in Figures 26 through 36. A bar velocity of 198,800 in/s is used in these calculations. This corresponds to a Young's modulus for steel of 29×10^6 lbs/in^2. This is considered a low but acceptable value for steel. However, the calculations still place the passbands at a slightly higher frequency than the data. Modification of the tool

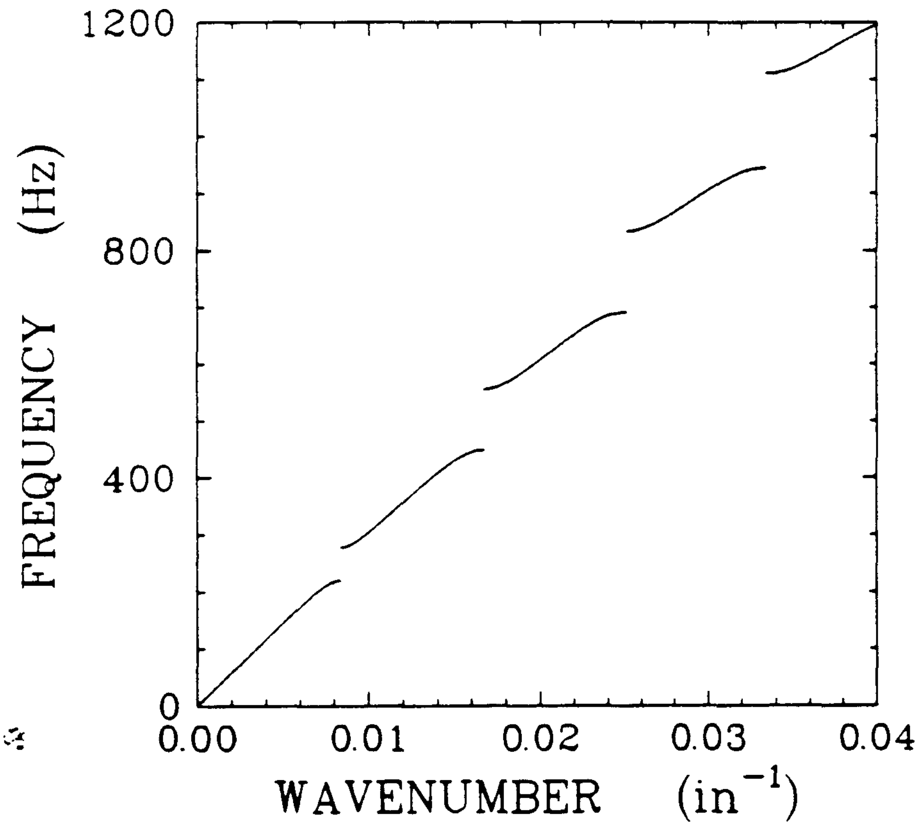

Figure 37: Theoretical Dispersion Curves for the Drill String.

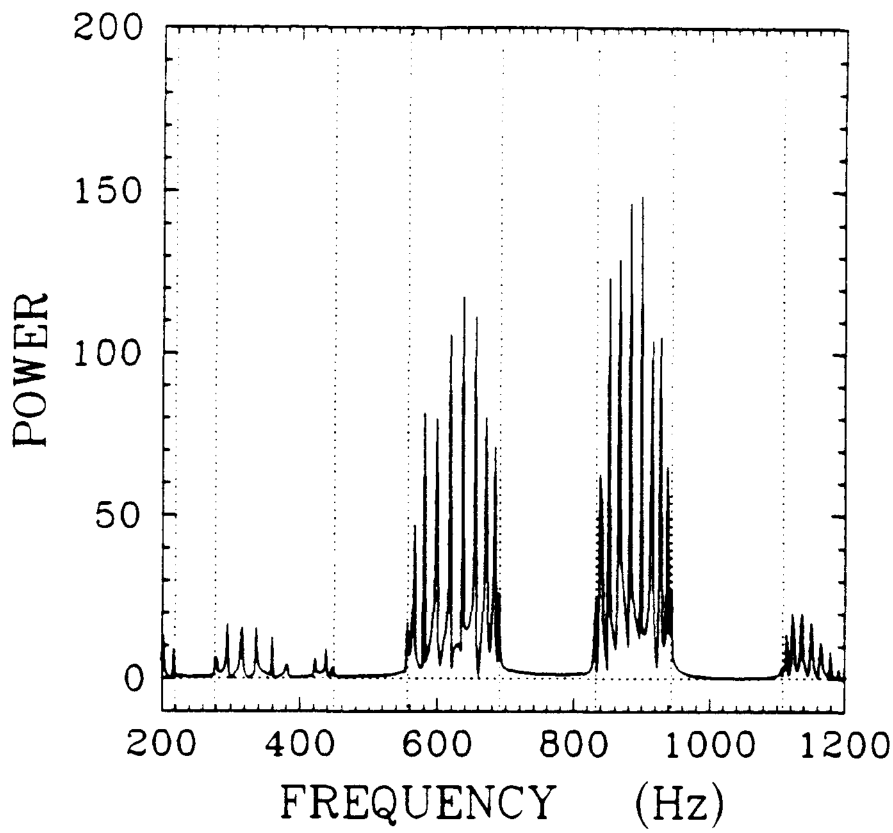

Figure 38: Theoretical Power Spectral Density of the 313-Ft Test. (The vertical dotted lines indicate the calculated boundaries of the passbands.)

joint dimensions cannot be used to improve this comparison, since the width as well as the position of the passband is affected.[8] However, even if a higher bar velocity for steel is used, 202,000 in/s corresponding to a modulus of 30×10^6 lbs/in^2, the correlation between these calculations and the field data is quite good.

A transient wave calculation can also be made using the analysis in Section 2.3. The 313-ft drill string is used for this calculation. Complete tool joints are placed at both ends of the drill string. The bottom boundary condition is a free surface. The top boundary condition is a displacement condition. The displacement profile at this boundary consists of two, 800 Hz oscillations followed by no motion. This is used to model the hammer blow as well as the effects of the cap and support structure. The recorded motion at the bottom of this system has the power spectrum shown in Figure 38. The essential features of the data spectrum shown in Figure 26 are present

[8]The data was recorded with a battery operated cassette recorder. No precautions were made to assure that the recorder was operating at the correct speed. A small increase in the tape speed could account for these discrepancies.

in this calculation. Note that ten spikes are present within the calculated passbands.

5 CONCLUSIONS

In this work the behavior of acoustical waves in a drill string has been investigated through theory, laboratory experiment, and field test. The objective of these studies is to determine the feasibility of using drill strings as an effective means of data transmission during drilling of oil, gas, and geothermal wells.

The theoretical analysis in Section 2 is based upon a method proposed by Brillouin [5]. This theory predicts the existence of a comb-filtering phenomena composed of alternating passbands and stopbands in frequency space. Superimposed on this banded structure are multiple spikes in the frequency spectrum resulting from standing wave effects. These effects are the result of echos between the opposite ends of the infinite length model.

Section 3 describes a 20th-scale model of a drill string which was tested for its acoustic transmission characteristics. The scale model was constructed of copper tube and has periodically spaced copper collars which represent the tool joints of a full-scale steel drill string. This scale model was subjected to an impulse load at one end, and the resulting longitudinal acoustic waves were measured at two locations. The data collected from this experiment exhibits all of the phenomena associated with wave propagation in a periodic structure. The one-dimensional theory developed in Section 2 was used to analyze the data. The correlation between theory and experiment was excellent.

In Section 4 the results of a field test reveal that all of the phenomena observed in the theory and the laboratory experiment are also relevant to the full-scale field environment. Possibly the most interesting point is that the standing-wave spikes were observed in this field test. The spikes could only have been produced by acoustical signals which propagated a minimum of 4700 ft in the drill string. This string was suspended in a mud-filled well and was undoubtedly in contact with the wall of the well at several locations.

It is concluded that the key problems associated with devising a method for telemetry of data by acoustical carrier waves in a drill string are suppression of echos and associated standing wave effects, and compensation for the phase distortion produced by wave dispersion within the passbands. Signal attenuation is not a major problem.

6 ACKNOWLEDGMENTS

I wish to express thanks to Robert D. Meyer and Thomas Schinke for assistance in the assembly of the experimental apparatus and the instrumentation. Several other people also contributed to this work. Thanks are given to Robert P. Wemple, John Gabaldon, and James E. Uhl.

I also wish to give special thanks to Preston Chaney for several interesting discussions about both the field test procedures and historical aspects of this problem. Upon retirement, he had the foresight to save a data tape which would otherwise have been lost. In addition he was gracious enough to allow me to use this tape for my analysis.

References

[1] William H. Cox and Preston E. Chaney, *Telemetry System*, U.S. Patent No. 4,293,936 (1981).

[2] H. Eugene Sharp and Miles A. Smither, *Borehole Acoustic Telemetry System with Phase Shifted Signal*, U.S. Patent No. 4,562,559 (1985).

[3] Clifford W. Petersen, John M. Bednar, Edwin J. Hocker, Jr., David H. Gauger, and James M. Henderson, *Acoustic Transmitter and Method to Produce Essentially Longitudinal, Acoustic Waves*, U.S. Patent No. 4,314,365 (1982).

[4] Thomas G. Barnes and Bill R. Kirkwood, *Passbands for Acoustic Transmission in an Idealized Drill String*, J. Acoust. Soc. Amer. 5, 1606-1608 (1972).

[5] Léon Brillouin, **Wave Propagation in Periodic Structures**, (Dover, New York, 1953).

[6] Anthony Bedford, Douglas S. Drumheller, and Herbert J. Sutherland, *On Modeling the Dynamics of Composite Materials*, **Mechanics Today, Vol. 3**, (Pergamon, New York, 1976), Edited by S. Nemat-Nasser.

[7] Courant, Friedricks, and Lewy, *On the Partial Difference Equations of Mathematical Physics*, Mathematische Annalen 100, 32 (1928). English translation: IBM Journal, March 1967.

[8] Ya. B. Zel'dovich and Yu. P. Raizer, **Physics of Shock Waves and High-Temperature Hydrodynamic Phenomena, Vol. 1**, (Academic Press, New York, 1966). Edited by Wallace D. Hayes and Ronald F. Probstein.

[9] **Drilling Data Handbook**, (Gulf Publishing Company, Houston, 1980).